ISSN 0030-6096

OSAKA CITY MEDICAL JOURNAL

Vol. 69
No. 2

2023

PUBLISHED BY
OSAKA CITY MEDICAL ASSOCIATION
OSAKA JAPAN

Osaka City Medical Journal
Vol. 69, No. 2, December 2023

CONTENTS

Osaka City Med. J. Vol. 69, 51-59, 2023

Analysis of Anti-laminin γ1 Autoantibodies in Anti-p200 Pemphigoid by Immunoblotting Using Cultured Cells

Daisuke Hayashi[1], Takashi Hashimoto[2], Mako Mine[2], Norito Ishii[3], Kentaro Izumi[4], and Daisuke Tsuruta[2]

Department of Dermatology[1], Graduate School of Medicine, Osaka City University; Department of Dermatology[2], Graduate School of Medicine, Osaka Metropolitan University; Department of Dermatology[3], Kurume University School of Medicine; and Department of Dermatology[4], Hokkaido University Graduate School of Medicine

Abstract

Background

Anti-p200 pemphigoid is a subepidermal autoimmune bullous disease involving IgG autoantibodies to the 200-kDa antigen. Although previous studies suggested that patient sera react with the 200-kDa laminin γ1, it is possible that another 200-kDa autoantigen is present. Here, we examined whether the anti-p200 pemphigoid patient sera react exclusively with laminin γ1 by performing experiments using *LAMC1*-knock-out (KO) cells produced by the use of CRISPR-Cas9.

Methods

We performed immunoblotting experiments using normal human dermal extract and extracts of various cultured cells, including *LAMC1*-KO HaCaT cells.

Results

While all the anti-p200 pemphigoid patient sera and the anti-laminin γ1 monoclonal antibody (mAb) reacted with the 200-kDa protein in normal human dermal extract, the mAb detected a smaller 190-kDa laminin γ1 molecule in extracts of various cultured cells. However, none of the patient sera reacted with the 190-kDa laminin γ1 in extracts of either intact or *LAMC1*-KO HaCaT cells.

Conclusions

We could not identify the 200-kDa antigen as laminin γ1 because the patient sera did not react with laminin γ1 in HaCaT cells. The reason may be that the 190-kDa laminin γ1 produced by the cultured cells lacks post-translational modifications necessary for autoantibody binding. However, this novel approach using the CRISPR-Cas9 technique should be useful for the identification of true autoantigens in patient sera that react with laminin γ1 in cultured cells.

Key Words: Anti-p200 pemphigoid; CRISPR-Cas9; HaCaT cell; Immunoblotting; Laminin γ1.

Received January 19, 2023; accepted March 3, 2023.

Correspondence to: Takashi Hashimoto, MD.
Department of Dermatology, Graduate School of Medicine, Osaka Metropolitan University, 1-4-3 Asahimachi, Abeno-ku, Osaka 545-8585, Japan
Tel: +81-6-6646-6630; Fax: +81-6-6646-6630
E-mail: hashyt@gmail.com

Introduction

Anti-p200 pemphigoid was first described in 1996 by Chen et al[1] and Zillikens et al[2] as a novel entity of subepidermal autoimmune bullous disease with IgG autoantibodies against an unknown 200-kDa antigen. Anti-p200 pemphigoid clinically shows blisters, erosions, and urticaria-like erythema, with a tendency to the development of smaller vesicles[3-7]. Mucosal lesions occasionally develop. The association with psoriasis has been reported in Japan and Asian countries, but not in European countries[3-7]. Histopathology shows subepidermal blisters and the inflammatory cell infiltrate of neutrophils and eosinophils in the upper dermis. Direct immunofluorescence (IF) shows linear IgG and C3 deposits at the basement membrane zone (BMZ). Indirect IF of normal human skin detects IgG anti-BMZ antibodies, which react with the dermal side of 1 M NaCl-split normal human skin. Immunoblotting of normal human dermal extracts detects a 200-kDa autoantigen.

In 2009, Dainichi et al identified the 200-kDa protein as laminin γ1 by proteomics[8]. In immunoblotting of normal human dermal extracts, they found that patient sera and an anti-laminin γ1 monoclonal antibody (mAb) reacted with the identical 200-kDa protein band. Furthermore, 90% of 32 patient sera reacted with recombinant laminin γ1 protein[8]. Another mAb, against the C-terminus of laminin γ1, competitively inhibited the reaction of patient sera with the p200 band in immunoblots of normal human dermal extract. Conversely, the IgG fraction purified from patient sera competitively inhibited the reactivity of the anti-laminin γ1 mAb in immunoblots of normal human dermal extract. From these results, Dainichi et al concluded that p200 is laminin γ1, and proposed the name anti-laminin γ pemphigoid for this disease[8].

Laminin γ1 is an N-linked glycoprotein with a molecular weight of 200 kDa[9-11]. In the skin, it forms heterotrimers such as laminins 311, 321, and 511, which are involved in epidermal and dermal binding outside the hemidesmosome. Shimanovich et al reported that anti-p200 pemphigoid sera react with an acidic noncollagenous N-linked glycoprotein of the cutaneous basement membrane[12], which suggests that the 200-kDa autoantigen may be one of the laminin γ subunits.

However, although laminin γ1 is also expressed in various tissues other than skin and mucosa[8], anti-p200 pemphigoid patients do not develop any lesions in other organs. Therefore, it is unclear why the autoantibodies in the patient sera react selectively with laminin γ1 in the skin. Dainichi et al speculated that the sera of anti-p200 pemphigoid patients might recognize laminin γ1 with skin-specific post-translational modifications and thus induce only the skin lesions[8]. However, the few attempts to unravel the pathogenic activity of anti-laminin γ1 antibodies have so far been unsuccessful[13-15]. Thus, it is still conceivable that, other than laminin γ1, there is an unknown 200-kDa autoantigen that might be the true pathogenic autoantigen.

Here, we examined whether the anti-p200 pemphigoid patient sera react truly and exclusively with laminin γ1. For this purpose, we generated laminin γ1-knock-out (KO) HaCaT cells and examined the reactivity of anti-p200 pemphigoid patient sera by immunoblotting of extracts of both the intact HaCaT cells and the *LAMC1*-KO HaCaT cells.

Methods

This study was approved by Ethics Committees of Osaka Metropolitan University (No. 2019-055), and adhered to Declaration of Helsinki principles.

Patient sera and normal control sera

We used 15 sera from anti-p200 pemphigoid patients; they were stored at the Department of

Dermatology, Osaka Metropolitan University, and the Department of Dermatology, Kurume University. All the patients fulfilled the following diagnostic criteria: linear deposits of IgG and/or C3 in the BMZ by direct IF, the presence of IgG anti-BMZ antibodies by indirect IF using normal human skin, positive IgG reactivity to the dermal side of 1 M NaCl-split normal human skin by indirect IF, and the detection of the 200-kDa antigen in immunoblots of normal human dermal extract. The sera were stored at −80℃ for the long term. When used for experiments, the sera were thawed and then stored again at −20℃ for further use. Normal sera from four volunteers were used as negative controls.

Production of a laminin γ1-KO HaCaT cell line by the use of CRISPR-Cas9

To establish a Cas9-expressing HaCaT cell line, HaCaT cells were infected with pLenti-EF1a-Cas9-Puro lentiviral particles (Applied Biological Materials Inc., Richmond, BC, Canada) according to the manufacturer's instructions. Using Lipofectamin RNAi Max (Thermo Fisher Scientific, Waltham, MA, USA), the cloned Cas9-expressing HaCaT cells were transfected with control gRNA (Integrated DNA Technologies, Coralville, IA, USA, Alt-R CRISPR-Cas9 Negative Control crRNA, 1072254) or gRNA targeting laminin γ1 (sequence: CTTAATCGCCTGAACACTTT) (Integrated DNA Technologies, Coralville, IA, USA), coupled to tracRNA (Integrated DNA Technologies, Coralville, IA, USA, 1075927). Subsequently, a *LAMC1*-KO HaCaT cell line was cloned.

Cell cultures

HaCaT cells (CLI Cell Lines Service, Eppelheim, Germany, 300493), DJM-1 cells, and SCC cells were cultured in Dulbecco's modified Eagle's medium (DMEM) (Fujifilm Wako Pure Chemical Corporation, Osaka, Japan, 04429765) supplemented with penicillin-streptomycin solution (Fujifilm Wako Pure Chemical Corporation, Osaka, Japan, 168-23191) and 5% filter-sterilized fetal bovine serum (FBS) (Thermo Fisher Scientific, Waltham, MA, USA, 10270106). Normal human epidermal keratinocytes (NHEKs) (Promo cell, Heidelberg, Germany, C12003) were cultured using keratinocyte growth medium (Promo cell, Heidelberg, Germany, C-20011). Normal human neonatal dermal fibroblasts (ATCC, Manassas, VA, USA, PCS-201-010) were cultured in fibroblast basal medium (ATCC, Manassas, VA, USA, PCS-201-030) supplemented with fibroblast growth kit-lower serum (ATCC, Manassas, VA, USA, PCS-201-041). The cell extracts were prepared by scraping the cells at 80%-90% confluency in SDS sample buffer for electrophoresis.

Indirect immunofluorescence analyses

Indirect immunofluorescence analyses of normal human skin and 1 M NaCl-split normal human skin were performed as previously described[3,8].

Immunoblot analysis

Running buffer for electrophoresis was prepared by adding MOPS running buffer 20×(Thermo Fisher Scientific, Waltham, MA, USA, NP0001) and 0.25% of antioxidant (Thermo Fisher Scientific, Waltham, MA, USA, NP0005) to distilled water. Next, 10 μL samples were applied to the lanes of a 3%-8% Tris-acetate gel (Thermo Fisher Scientific, Waltham, MA, USA, EA0375BOX) and were electrophoresed at 200 V for 1 h. The proteins in the gel were transferred to PVDF membrane (Bio-Rad Laboratories, Inc. Hercules, CA, USA, cat #1704156). The membranes were then blocked with 3% skim milk in PBS for 1 h, and washed with PBS with 0.5% Tween-20 in PBS (PBS-T) for 10 min, 3 times.

As primary antibodies, patient sera were diluted 1:5 in 3% skim milk in PBS, and the anti-laminin γ1 mouse IgG monoclonal antibody (mAb) (Atlas Antibodies, Stockholm, Sweden, AMAb91137) was used at 1:1000-1:10000 dilutions in 3% skim milk in PBS. Primary antibodies were incubated overnight at 4℃ and the membranes were then washed for 10 min 3 times in PBS-T. The blots were

then incubated with secondary antibodies, HRP-anti-human IgG antibody (Agilent Technologies Dako, Glostrup, Denmark, P0214) at 1:1000 dilution and HRP-anti-mouse IgG antibody (SouthernBiotech, Birmingham, AL, USA, 1031-05) at 1:5000 dilution, for 1 h at room temperature, and then washed for 10 min 3 times in PBS-T. Positive reactivity was detected with an Image Quant LAS 4000 (GE Healthcare, Chicago, IL, USA) using Super Signal (Thermo Fisher Scientific, Waltham, MA, USA). We used of the same patients' sera as representative in all the experiments.

Results

Indirect immunofluorescence analyses of anti-p200 pemphigoid patient sera

By indirect immunofluorescence of normal human skin, all 15 anti-p200 pemphigoid patient sera showed anti-BMZ antibodies that reacted with the dermal side of split skin (Fig. 1, the results of 3 representative sera are shown).

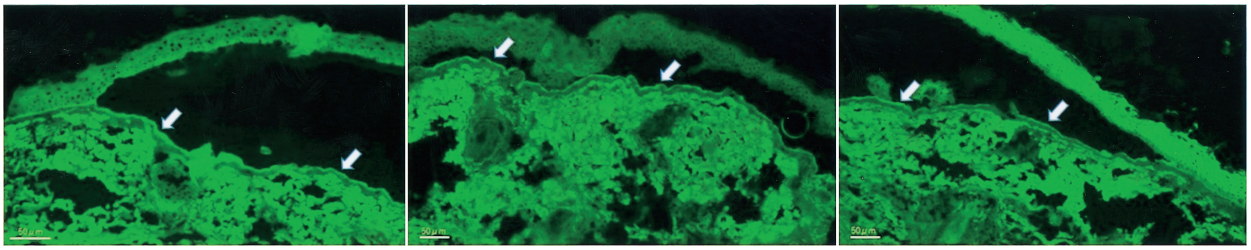

Figure 1. Indirect immunofluorescence of 1 M NaCl-split normal human skin using 3 representative anti-p200 pemphigoid sera (patients1-3). White arrows indicate the reactivity with the dermal side of the split.

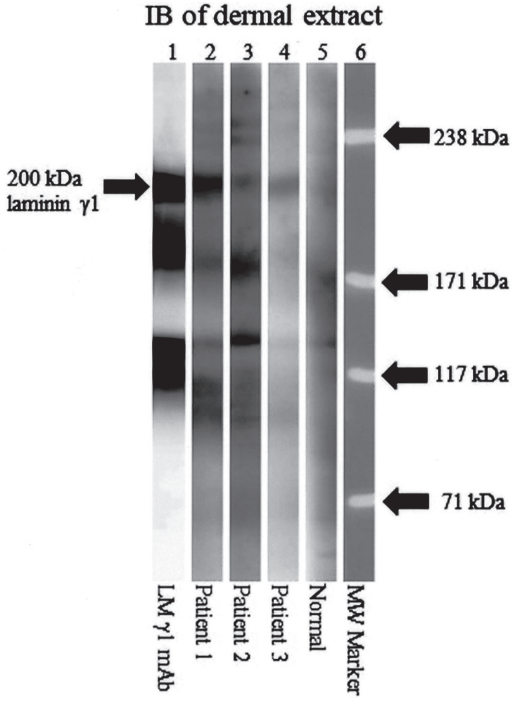

Figure 2. Immunoblotting of normal human dermal extract using 3 representative anti-p200 pemphigoid sera. Anti-laminin γ1 mAb reacted with the 200-kDa laminin γ1 (lane 1). The same 200-kDa protein also reacted with the 3 representative anti-p200 pemphigoid patient sera (patients 1-3), but not with normal control serum (lane 5). The 238- and 171-kDa bands of the molecular weight (MW) markers (lane 6) are indicated by arrows on the right.

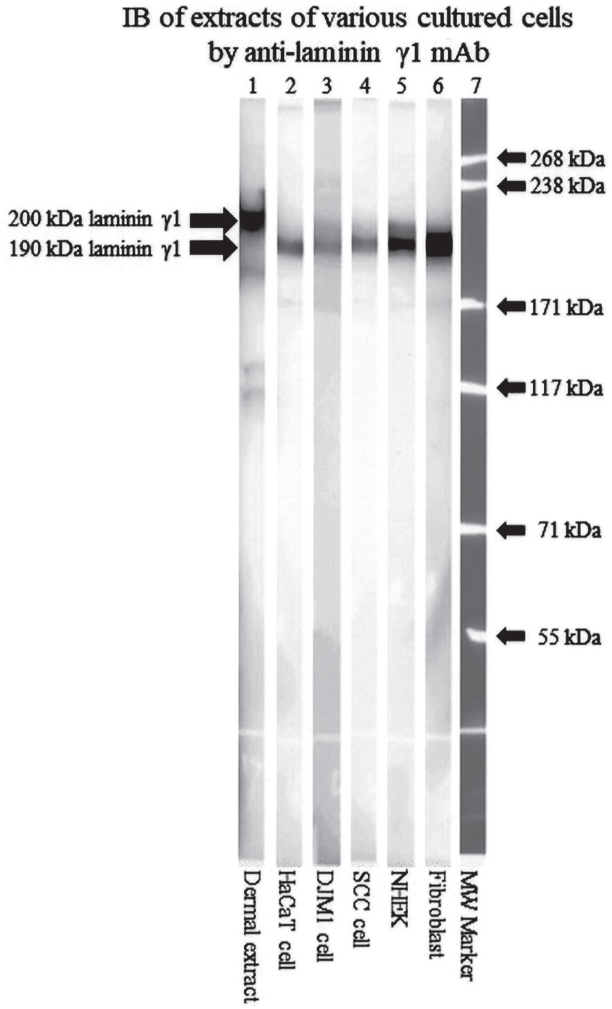

Figure 3. Immunoblotting of extracts of various cultured cells with the anti-laminin γ1 mAb. While this mAb reacted with the 200-kDa laminin γ1 in normal human dermal extracts (lane 1), it reacted with the 190-kDa laminin γ1 in all the cultured cells, including HaCaT cells (lane 2), DJM-1 cells (lane 3), SCC cells (lane 4), normal human epidermal keratinocytes (NHEKs) (lane 5), and dermal fibroblasts (lane 6). The 238- and 171-kDa bands of the molecular weight (MW) markers (lane 7) are indicated by arrows on the right.

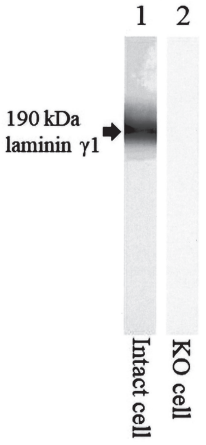

Figure 4. Immunoblotting of extracts of intact HaCaT cells and *LAMC1*-KO HaCaT cells with anti-laminin γ1 mAb. The mAb reacted with the 190-kDa laminin γ1 in intact HaCaT cell extract (lane 1), and did not detect it in *LAMC1*-KO HaCaT cell lysate (lane 2).

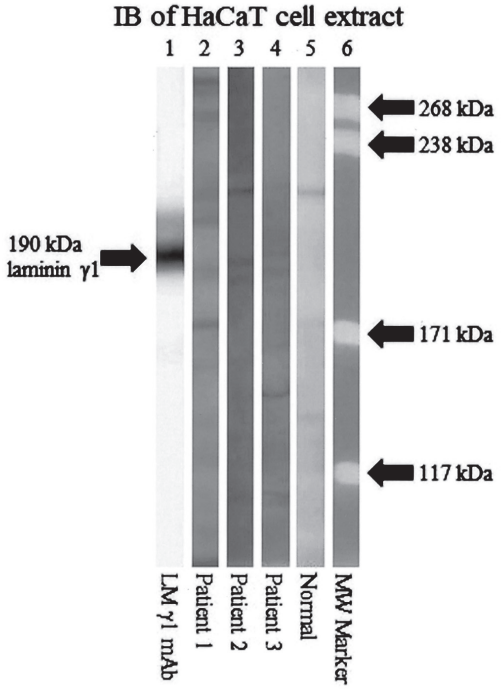

Figure 5. Immunoblotting of extracts of intact HaCaT cells with anti-p200 pemphigoid patient sera. While the anti-laminin γ1 mAb detected the 190-kDa laminin γ1 (lane 1), this band was not detected by any of the 3 representative anti-p200 pemphigoid patient sera (lane 2-4) or by normal serum (lane 5). The 238- and 171-kDa bands of the molecular weight (MW) markers are indicated by arrows on the right (lane 6).

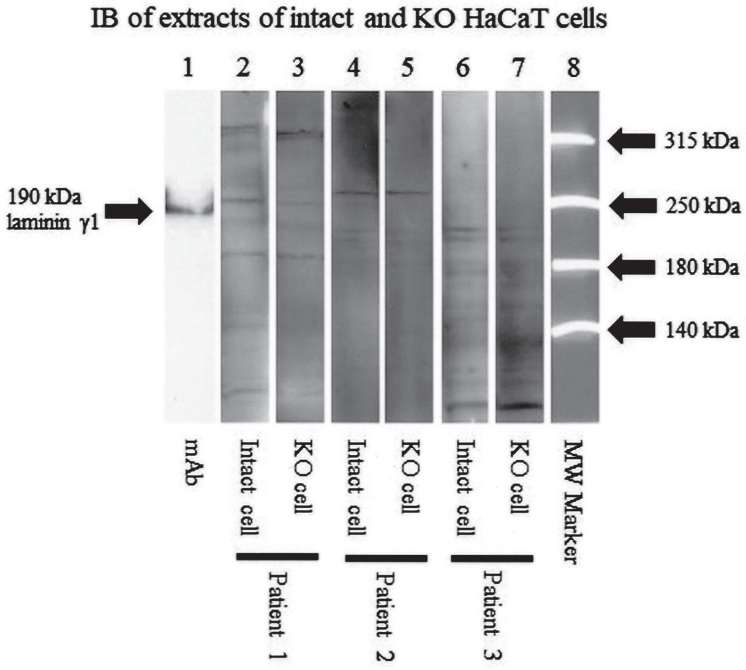

Figure 6. Immunoblotting of extracts of intact HaCaT cells and *LAMC1*-KO HaCaT cells with anti-p200 pemphigoid patient sera. The anti-laminin γ1 mAb reacted with the 190-kDa laminin γ1 in intact HaCaT cell extract (lane 1), but was not detected by any of the 3 representative anti-p200 pemphigoid patient sera in extracts of either intact HaCaT cells or *LAMC1*-KO HaCaT cells (lanes 2-7). The 250- and 180-kDa bands of the molecular weight (MW) markers are indicated by arrows on the right (lane 8).

Immunoblotting of normal human dermal extract with anti-p200 pemphigoid patient sera

In immunoblots of normal human dermal extract, all 15 anti-p200 pemphigoid patient sera reacted with the 200-kDa protein band (Fig. 2, the results of 3 representative sera are shown), which was also strongly detected by the anti-laminin γ1 mAb.

Immunoblotting of extracts of various cultured cells by anti-laminin γ1 mAb

To confirm their expression of laminin γ1, we performed immunoblotting with extracts of various cultured cells, including HaCaT cells, DJM1 cells, SCC cells, NHEKs, and dermal fibroblasts, using anti-laminin γ1 mAb. While the anti-laminin γ1 mAb detected the 200-kDa laminin γ1 in normal human dermal extract (Fig. 3, lane 1), the mAb reacted with an approximately 190-kDa smaller laminin γ1 in the extracts of all the other cultured cells (Fig. 3, lanes 2-6).

Immunoblotting of intact HaCaT cell extract and LAMC1-KO HaCaT cell extracts with anti-laminin γ1 mAb

To confirm the lack of p200 detection in *LAMC1*-KO HaCaT cells, we compared the laminin γ1 reactivity of intact HaCaT cells and *LAMC1*-KO HaCaT cells by immunoblotting. The anti-laminin γ1 mAb detected the 190-kDa laminin γ1 in immunoblots of intact HaCaT cells, but did not detect it in *LAMC1*-KO HaCaT cell extract (Fig. 4), confirming that laminin γ1 was knocked out in the *LAMC1*-KO HaCaT cells.

Immunoblotting of intact HaCaT cell extract and LAMC1-KO HaCaT cell extracts with anti-p200 pemphigoid patient sera

Next, we performed immunoblotting of intact HaCaT cell extract with all 15 anti-p200 pemphigoid patient sera. However, although the anti-laminin γ1 mAb detected the 190-kDa laminin γ1 in immunoblots of extracts of intact HaCaT cells, none of the patient sera detected the 190-kDa protein band in intact HaCaT cell extract (Fig. 5, the results of 3 representative sera are shown). In further immunoblotting of extracts of both intact HaCaT cells and *LAMC1*-KO HaCaT cells, the 190-kDa protein band was not detected in either extract by any of the 15 anti-p200 pemphigoid patient sera (Fig. 6, the results of 3 representative sera are shown).

Discussion

The aim of this study was to examine whether the anti-p200 pemphigoid sera really and exclusively react with laminin γ1.

First, we confirmed the reactivity of all the 15 anti-p200 pemphigoid sera with the 200-kDa p200 by indirect immunofluorescence of 1 M NaCl-split skin and immunoblotting of normal human dermal extract. The results confirmed the results of the previous studies by Li et al[11].

The first important result in this study was that, by immunoblotting analysis of extracts of various cultured cells using anti-laminin γ1 mAb, all the cultured cells, including HaCaT cells, DJM1 cells, SCC cells, NHEKs, and dermal fibroblasts, expressed laminin γ1 molecules of approximately 190 kDa, which were smaller than the 200-kDa laminin γ1 in human dermal extract.

In the next experiment, we successfully produced a *LAMC1*-KO HaCaT cell line, using CRISPR-Cas9. Its lack of laminin γ1 expression was confirmed by immunoblotting with the anti-laminin γ1 mAb.

Next, we examined the 15 patient sera by immunoblotting extracts of both the intact HaCaT cells and the *LAMC1*-KO HaCaT cells. However, none of the patient sera showed positive reactivity with the 190-kDa laminin γ1 in either extract. Thus, we could not confirm that all the patient sera really

reacted with laminin γ1 with this approach.

The reason for the negative reactivity of patient sera with the smaller 190-kDa laminin γ1 in HaCaT cells is currently unknown. However, it is conceivable that the cultured cells could not produce enough post-translational modifications with which the anti-laminin γ1 autoantibodies in the patient sera react. This speculation is supported by previous reports that N-linked glycosylation of laminin γ1 influences its recognition by anti-p200 pemphigoid autoantibodies[11,12].

The present results also suggest that other target proteins may be present.

Conclusions

In this study, we could not identify the 200-kDa antigen as laminin γ1 because the patient sera did not react with laminin γ1 in either intact or *LAMC1*-KO HaCaT cells. However, this approach using the CRISPR-Cas9 technique should be useful in identifying true autoantigens in patient sera that react with laminin γ1 in cultured cells. Future studies to clarify the nature of the pathogenic autoantibodies in anti-p200 pemphigoid, and particularly to attempt to identify any different autoantigen, are warranted.

Acknowledgements

All authors have no COI to declare regarding the present study.

We thank Ms. Nami Ikeshita, Department of Dermatology, Hokkaido University Graduate School of Medicine, for her technical assistance. We are grateful to Ms. Noriko Okabayashi and Ms. Yoko Mukaoku, Graduate School of Medicine, Osaka Metropolitan University, for their secretarial work. We thank all the patients for their participation. We are grateful to Dr. Xiaoguang Li and Dr. Hua Qian, Department of Laboratory Medicine, Medical College, Dalian University, Dalian, China, for critically reading and commenting on the manuscript.

Grants: This study was supported by JSPS KAKENHI Grant (Grant-in-Aid for Scientific Research (C)) (Number 21K08331) to Takashi Hashimoto, by "Research on Measures for Intractable Diseases" from the Ministry of Health, Labor and Welfare Project to Takashi Hashimoto, and by grants from Takeda Science Foundation, and AbbVie GK.

References

1. Chen KR, Shimizu S, Miyakawa S, et al. Coexistence of psoriasis and an unusual IgG-mediated subepidermal bullous dermatosis: identification of a novel 200-kDa lower lamina lucida target antigen. Br J Dermatol 1996; 134:340-346.
2. Zillikens D, Kawahara Y, Ishiko A, et al. A novel subepidermal blistering disease with autoantibodies to a 200-kDa antigen of the basement membrane zone. J Invest Dermatol 1996;106:465-470.
3. Hashimoto T, Tsuruta D, Koga H, et al. Summary of results of serological tests and diagnoses for 4774 cases of various autoimmune bullous diseases consulted to Kurume University. Br J Dermatol 2016;175:953-965.
4. Dainichi T, Koga H, Tsuji T, et al. From anti-p200 pemphigoid to anti-laminin gamma1 pemphigoid. J Dermatol 2010;37:231-238.
5. Goletz S, Hashimoto T, Zillikens D, et al. Anti-p200 pemphigoid. J Am Acad Dermatol 2014;71:185-191.
6. Kridin K, Ahmed AR. Anti-p200 pemphigoid: a systematic review. Front Immunol 2019;10:2466.
7. Solimani F, Pollmann R, Ishii N, et al. Diagnosis of anti-laminin γ-1 pemphigoid by immunoblot analysis. J Eur Acad Dermatol Venereol 2019;33:735-741.
8. Dainichi T, Kurono S, Ohyama B, et al. Anti-laminin gamma-1 pemphigoid. Proc Natl Acad Sci U S A 2009;106: 2800-2805.
9. Ido H, Nakamura A, Kobayashi R, et al. The requirement of the glutamic acid residue at the third position from

the carboxyl termini of the laminin gamma chains in integrin binding by laminins. J Biol Chem 2007;282: 11144-11154.
10. Taniguchi Y, Ido H, Sanzen N, et al. The C-terminal region of laminin beta chains modulates the integrin binding affinities of laminins. J Biol Chem 2009;284:7820-7831.
11. Li X, Qian H, Takizawa M, et al. N-linked glycosylation on laminin γ1 influences recognition of anti-laminin γ1 pemphigoid autoantibodies. J Dermatol Sci 2015;77:125-129.
12. Shimanovich I, Hirako Y, Sitaru C, et al. The autoantigen of anti-p200 pemphigoid is an acidic noncollagenous N-linked glycoprotein of the cutaneous basement membrane. J Invest Dermatol 2003;121:1402-1408.
13. Vafia K, Groth S, Beckmann T, et al. Pathogenicity of autoantibodies in anti-p200 pemphigoid. PLoS One 2012; 7:e41769.
14. Koga H, Ishii N, Dainichi T, et al. An attempt to develop mouse model for anti-laminin γ1 pemphigoid. J Dermatol Sci 2013;70:108-115.
15. Florea F, Bernards C, Caproni M, et al. Ex vivo pathogenicity of anti-laminin γ1 autoantibodies. Am J Pathol 2014;184:494-506.

Osaka City Med. J. Vol. 69, 61-65, 2023

Prolonged Olfactory Dysfunction in the COVID-19 Era; Etiological Analysis in a Single-centered Cohort

Hiroko Kawai[1)], Kousuke Hashimoto[1)], Yuichi Teranishi[1)], Yu Nakagama[2,3)], Yasutoshi Kido[2,3)], and Kishiko Sunami[1)]

Departments of Otolaryngology[1)], Virology & Parasitology[2)], and Research Center for Infectious Disease Sciences[3)], Graduate School of Medicine, Osaka Metropolitan University

Abstract

Background

The prognosis of olfactory dysfunction (OD) is variable, largely depending on the etiology. The coronavirus disease 2019 (COVID-19)-related OD tends to resolve within a few weeks; however, 10%-15% of the patients suffer prolonged OD (POD) persisting beyond the first month. This study aimed to determine the disease burden of COVID-19 in patients with undiagnosed POD and compare the characteristics of COVID-19-related POD with other PODs.

Methods

Patients with POD (>4 weeks) visiting our outpatient clinic between December 2020 and January 2022 were analyzed to include their clinical data, laboratory variables, endoscopy and computed tomography findings. COVID-19 was detected using serological testing; OD severity was assessed using the Self-Administered Odor Questionnaire, the Open Essence, and intravenous olfactometry. Characteristics of patients with and without COVID-19 were compared.

Results

Sixteen patients (11 females; median age: 42 [15-83] years) were included, of which nine were serologically positive for COVID-19. Compared with other etiologies, COVID-19-related POD was more commonly sudden onset and presented with gustatory and intranasal trigeminal dysfunction (assessed by the patient's inability to identify the cooling sensation elicited by menthol). Some patients had discrepancies between the change in subjective symptoms and test results; however, most COVID-19-related POD patients showed improvement.

Conclusions

The overall burden of POD increased significantly due to the COVID-19 pandemic. Accordingly, OD should be assessed using plural subjective tests. Further research using larger samples and targeting different coronavirus variants is required to corroborate these results.

Key Words: Olfactory dysfunction; COVID-19; Serological test

Received December 20, 2022; accepted April 11, 2023.

Correspondence to: Hiroko Kawai, MD.
Department of Otolaryngology, Head and Neck Surgery, Graduate School of Medicine, Osaka Metropolitan University, 1-4-3 Asahimachi, Abeno-ku, Osaka 545-8585, Japan
Tel: +81-6-6645-3871; Fax: +81-6-6645-0515
E-mail: c21736w@omu.ac.jp

Introduction

Prolonged olfactory dysfunction (POD) can be triggered by various etiologies, including airway obstruction and neural disorders, although viral diseases are common cause. The recent coronavirus disease 2019 (COVID-19) was primarily characterized by impaired olfaction, contributing to an overall increase in the prevalence of POD; however, the exact extent is still unknown. Although COVID-19-related olfactory dysfunction (OD) was initially considered to have a good prognosis; resolve within a few weeks, recent long-term follow-up reports estimate a significant proportion of patients with COVID-19-related olfactory impairment to develop POD (1%-48%)[1,2]. In addition, we supposed that there were some POD patients who were not able to receive a diagnosis, because the inspection system was insufficient just after the COVID-19 pandemic in Japan. Therefore, this study aimed to evaluate the relative burden of COVID-19 disease in a single-center cohort of patients diagnosed with a POD of previously undetermined etiology. The clinical characteristics of COVID-19-related POD were compared with that caused by other etiologies.

Methods

This study is a cross-sectional study, in a single cohort, which considered about the association between the clinical characteristics and the progress of OD and COVID-19 infection. The Strengthening the Reporting of Observation Studies in Epidemiology statement guidelines[3] were followed while reporting the findings.

Patients who visited the outpatient clinic at the Department of Otolaryngology, Osaka Metropolitan University Hospital, Japan, between December 2020 and January 2022 for self-reported prolonged (lasting >4 weeks) impairment in sense of smell were included in the study. Clinical data regarding symptoms, laboratory variables, endoscopy and computed tomography (CT) findings, and final diagnosis, were extracted from medical records. This study was approved by the institutional review board of the Osaka Metropolitan University (approval number: 2020-162). All participants provided informed consent to participate.

To determine the etiology of their POD, participants were tested for anti-severe acute respiratory syndrome coronavirus-2 (SARS-CoV-2) antibodies using the Elecsys Anti-SARS-CoV-2 assay (Roche, Basel, Switzerland). Participants with positive serology against SARS-CoV-2 were diagnosed with COVID-19-related POD. Additionally, CT was used to diagnose paranasal sinus abnormalities. Those testing negative for SARS-CoV-2 were categorized either as non-SARS-CoV-2 post-viral POD (persistent olfactory sensation impairment after recovery from acute rhinitis) or idiopathic POD.

The pattern and severity of olfactory sense impairment were assessed in almost all patients both qualitatively and quantitatively using the following methods: (i) Self-Administered Odor Questionnaire (SAOQ) developed by the Japan Rhinology Society to assess an individual's ability to identify 20 different odorants[4]. (ii) The Open Essence (OE) smell identification card to assess an individual's ability to identify 12 different odorants familiar to the Japanese population[5]. Menthol, an OE odorant, stimulates intranasal trigeminal system. (iii) Intravenous olfactometry (IO) to measure the latency in recognizing garlic-like odors and perception duration after an injection of thiamine propyl-disulfide. For the SAOQ and OE, the percentage of correct answers indicated the degree of impairment. The participants who were available for the follow-up underwent the SAOQ or OE tests again when more than one month has passed since the first visitation of our hospital. Moreover, the participants underwent medical examination and interview by an otolaryngologist

whenever they visited the hospital.

We compared outcomes (SAOQ, IO, and OE) between the two groups, COVID-19-related POD and non-COVID-19-related POD. SAOQ, IO, and total point of OE were compared using Mann-Whitney U test. The ability to recognize menthol was compared using Chi-square test. A two-sided $p < 0.05$ was considered statistically significant.

Results

We considered 16 patients, (11 females, 69%) with a median age of 42 years (interquartile range: 15-83 years). Nine of the 16 patients (56%) were serologically positive for COVID-19-related POD. One participant with a 'high-negative' result was further tested using the Architect SARS-CoV-2 IgG and IgG Ⅱ Quant (Abbott, Chicago, Illinois, USA) immunoassays targeting nucleocapsid and spike proteins, respectively. In the absence of a SARS-CoV-2 vaccination, the participant had 'positive' results on both confirmatory immunoassays and was, thus, classified as having a positive serology. Seven of the nine serological positive participants lacked an acute diagnosis of COVID-19. Other causes of POD included eosinophilic sinusitis (n=1), non-SARS-CoV-2 post-viral (n=2), and idiopathic (n=4). A comparison of clinical characteristics between patients of COVID-19- related POD and POD from other etiologies is given in Table1. In one of COVID-19-related POD patient, the SAOQ and OE tests were not performed, and another one patient dropped out of the study.

Patients diagnosed with COVID-19-related POD were more likely to experience gustatory dysfunction than those with an other-cause POD (n=6/9, 67% vs n=2/7, 29%). Although statistically non-significant, POD severity assessed using all three methods tended to increase with COVID-19-related disease severity of first assessment (median SAOQ: 8.1 vs 16.8; median OE: 4.1 vs 5.9; median latency of IO: 24.7 vs 14.0). Furthermore, on comparing the impairment patterns of OE odor

Table 1. Demographic and clinical variables of participants with prolonged olfactory dysfunction

	COVID-19-related (n=8)	Other miscellaneous (n=7)	p-value
Age, years (mean±SD)	37.1±20.0	47.7±18.6	
Female sex, n (%)	6 (67%)	5 (71%)	
Accompanying symptoms, n (%)			
Gustation dysfunction	6 (67%)	2 (29%)	
Dry cough	1 (11%)	0 (0%)	
Nasal obstruction	0 (0%)	1 (14%)	
None	2 (22%)	4 (57%)	
Imaging abnormalities, n (%)	0 (0%)	1 (14%)	
SAOQ, % (mean±SD)	8.1±10.1	16.8±15.4	p=0.22
IO, seconds (mean±SD)			
Latency	24.7±15.0	14.0±8.2	
Duration	50.2±45.7	49.4±41.8	
OE, points (mean±SD)			
Total	4.1±2.6	5.9±4.4	p=0.36
Menthol (Trigeminal dysfunction)	4 (50%)	2 (29%)	p=0.46
Other	3.6±2.3	5.1±4.1	
Prognosis			
Improvement	7 (87.5%)	3 (42.9%)	p=0.11
No change	1 (12.5%)	4 (57.1%)	

Table 2. The clinical characteristics of COVID-19-related POD patients. Duration shows the time to first visitation of our hospital from the onset of OD.

	Sex	Age (years)	Onset	Duration (weeks)	Accompany symptoms	OE (points)	SAOQ (points)	Prognosis
Case1	Female	56	After nasal congestion	12	Gustatory dysfunction	0	0	Improvement
Case2	Female	15	Suddenly	28	None	1	4	Improvement
Case3	Female	17	Suddenly	20	Gustatory dysfunction	5	27	Improvement
Case4	Female	46	Suddenly	8	Gustatory dysfunction	4	0	Improvement
Case5	Female	58	Suddenly	20	Gustatory dysfunction	8	20	Improvement
Case6	Male	16	Suddenly	16	Gustatory dysfunction	4	2	Improvement
Case7	Female	25	Suddenly	4	Dry cough	6	9	Drop out
Case8	Male	35	Suddenly	8	Gustatory dysfunction	5	3	Improvement
Case9	Male	66	Suddenly	56	None	None	None	No change

discrimination evaluated for different odorants, about half of the patients (n=4) with COVID-19 were not able to recognize the cooling sensation of menthol was higher as compared to only 29% (n=2/7) of those with POD from other causes. In contrast, COVID-19-related POD had a better prognosis than other PODs (n=7/8, 87.5% vs n=3/4). They showed partial improvement by SAOQ, OE, and interview.

Table 2 presents details of patients with COVID-19-related POD. Eight out of nine patients with COVID-19 POD experienced sudden onset of olfactory impairment; most of our patients were females aged <40 years. The severity of olfactory impairment was variable across the patients; Case3, 4, 6, and 8 had discrepancies between the result of OE and SAOQ, but seven of the eight patients reported partial improvement. Case 5 and 8 received nucleic acid amplification test before the visiting our hospital.

Discussions

In the contemporary COVID-19 era, the burden of POD of Osaka has surprisingly doubled, which highlights the considerable threat posed by COVID-19-related POD on the quality of life patients as well as the Japanese public health system. Surprisingly, seven of the nine patients with COVID-19 lacked an acute diagnosis and were later diagnosed serologically, which reflects the ground situation in Japan of a severe shortage of molecular diagnostics. Other report showed that 20% had IgG antibodies, whereas those without a positive COVID-19 diagnosis, and olfactory or gustatory dysfunction were the least prevalent in the population without a COVID-19 diagnosis like a symptom of fever[6]. The existing evidence corroborating the seroprevalence of COVID-19-related impairment in olfactory sensations used a subjective assessment of the extent of impairment and lacked quantitative data to substantiate these findings[7]. Our findings confirmed the previously reported magnitude of increased disease burden, using robust indices of qualitative and quantitative analysis (SAOQ, OE,

and IO), and medical examination by an otolaryngologist.

Like the gustatory system, the intranasal trigeminal system is also recognized as a common neuronal target of the SARS-CoV-2[8]. OE, widely used testing method in Japan, comprises menthol as one of the 12 odorants used to screen any coexisting intranasal trigeminal dysfunction. Non-recognition of the cooling sensation of menthol might indicates a trigeminal dysfunction, which was more commonly observed in our patients with COVID-19-related POD. It was suggested that accompanying intranasal trigeminal dysfunction had relevance to POD[9]. However, some patients reported a subjective improvement in POD during interviews, despite an inconsistent improvement in OE scores. This discrepancy could be attributed to the patient's inability to distinguish trigeminal sensation from olfaction. Furthermore, it is difficult to evaluate olfactory dysfunction (OD) based solely on subjective self-reporting, which was observed as the discrepancy in OE and SAOQ results of the same patient. Thus, multiple approaches, including diagnostic interviews, OE and SAOQ, should be used in assessing POD clinically.

This study has some limitations. First, the sample size was small and based on single center; therefore, we could not obtain statistically significant differences. Second, we did not differentiate between SARS-CoV-2 variants have been reported so far with only a few differences in demographic and symptoms. Future studies should include a large sample size and examine the differences based on the disease variant to corroborate these results.

Acknowledgement

All authors have no COI to declare regarding the present study.

YN and YK report ownership of equity of Quantum Molecular Diagnostics, an Osaka Metropolitan University spinout. YN and YK receive financial support outside the work from Abbott Japan LLC.

The sponsor had no control on the writing and publication of this study.

We gratefully acknowledge work of members of our laboratory and thank Enago (www.enago.jp) for the English language review.

References

1. Paderno A, Mattavelli D, Rampinelli V, et al. Olfactory and gustatory outcomes in COVID-19: a prospective evaluation in nonhospitalized subjects. Otolaryngol Head Neck Surg 2020;163:1144-1149.
2. Biadsee A, Dagan O, Ormianer Z, et al. Eight-month follow-up of olfactory and gustatory dysfunctions in recovered COVID-19 patients. Am J Otolaryngol 2021;42:103065.
3. von Elm E, Altman DG, Egger M, et al. The Strengthening the Reporting of Observational Studies in Epidemiology (STROBE) Statement: guidelines for reporting observational studies. Int J Surg 2014;12:1495-1499.
4. Takebayashi H, Tsuzuki K, Oka H, et al. Clinical availability of a self-administered odor questionnaire for patients with olfactory disorders. Auris Nasus Larynx 2011;38:65-72.
5. Nishida K, Kobayashi M, Ogihara H, et al. Clinical usefulness of smell identification test card: Open Essence. Nihon Jibiinkoka Gakkai Kaiho 2010;113:751-757. (In Japanese)
6. Bühler KM, Echeverry-Alzate V, Calleja-Conde J, et al. Seroprevalence of anti-SARS-CoV-2 IgG antibodies: relationship with COVID-19 diagnosis, symptoms, smoking, and method of transmission. IJID Reg 2022;4:10-16.
7. Makaronidis J, Mok J, Balogun N, et al. Seroprevalence of SARS-CoV-2 antibodies in people with an acute loss in their sense of smell and/or taste in a community-based population in London UK: an observational cohort study. PLos Med 2020;17:e1003358.
8. Green BG. Surveying chemosensory dysfunction in COVID-19. Chem Senses 2020;45:509-511.
9. Ferreli F, Bari MD, Gaino F, et al. Trigeminal features in COVID-19 patients with smell impairment. Int Forum Allergy Rhinol 2021;11:1253-1255.

Osaka City Med. J. Vol. 69, 67-74, 2023

Outcomes of COVID-19 Pneumonia Patients Complicated with Barotrauma under Mechanical Ventilation

Masahiro Miyashita, Ryo Deguchi, Seiya Kurimasa, Fumiaki Wakita, Hoshi Himura, Akihiro Kawamoto, Kenichiro Uchida, Tetsuro Nishimura, Hiromasa Yamamoto, and Yasumitsu Mizobata

Department of Traumatology and Critical Care Medicine, Graduate School of Medicine, Osaka Metropolitan University

Abstract

Background

In the treatment of severe COVID-19 pneumonia, we often experience patients with pneumothorax or pneumomediastinum. Complications of such barotrauma make respiratory treatments using mechanical ventilation more complicated and difficult. The purpose of this study was to evaluate the incidence and mortality of barotrauma in patients with severe COVID-19 pneumonia and to clarify the related factors and the effect of therapy.

Methods

From April 2020 to May 2021, 129 patients with severe COVID-19 pneumonia were treated with mechanical ventilation in the intensive care unit of the Emergency Critical Care Center of Osaka City University Hospital. After tracheal intubation, patients were mechanically ventilated under pressure control mode that kept peak inspiratory pressure below 30 cmH_2O. A muscle relaxant drug was administered for 48 hours after tracheal intubation, and airway occlusion pressure was monitored to minimize patient self-inflicted lung injury. We retrospectively investigated the incidence of barotrauma and mortality of the patients.

Results

Barotrauma occurred in 11 patients (8.5%), 5 with pneumothorax alone, 4 with pneumomediastinum alone, and 2 patients with both. The overall mortality rate of the 129 patients with severe COVID-19 pneumonia was 23%, but that of the patients complicated with barotrauma was 73%.

Conclusions

The incidence of barotrauma in severe COVID-19 pneumonia at our hospital was low compared with that of previous reports. Precise management of mechanical ventilation with strict prevention of patient self-inflicted lung injury might be one of the factors leading to this low incidence rate.

Key Words: Barotrauma; COVID-19; Pneumonia; Pneumothorax; Pneumomediastinum

Received August 2, 2022; accepted June 13, 2023.

Correspondence to: Masahiro Miyashita, MD.
Department of Trauma and Critical Care Medicine, Graduate School of Medicine, Osaka Metropolitan University, 1-4-3 Asahimachi, Abeno-ku, Osaka 545-8585, Japan
Tel: +81-6-6645-2121; Fax: +81-6-6645-3986
E-mail: miya@omu.ac.jp

Introduction

Since the beginning of 2020, Coronavirus disease-2019 (COVID-19) pneumonia has spread rapidly all over the world. In Japan, patients with severe COVID-19 were transferred to designated hospitals by the government. Osaka City University Hospital, one of these designated hospitals, thus started to treat the patients with severe COVID-19 pneumonia who required mechanical ventilation due to hypoxemia under oxygen therapy.

Patients with severe COVID-19 pneumonia mainly present with acute respiratory distress syndrome (ARDS), and we often treat these patients with a high positive end-expiratory pressure (PEEP) ventilator setting to prevent alveolar collapse. However, increased airway pressure may cause ventilator-related lung damage, leading to pneumothorax and pneumomediastinum. Patients who develop such barotrauma require more careful control of airway pressure, which makes their treatment more difficult.

The purpose of this study was to investigate the incidence and mortality of barotrauma in patients with severe COVID-19 pneumonia and to clarify the related factors and the effects of therapy.

Methods

We retrospectively investigated the medical records of 129 patients with severe COVID-19 pneumonia treated using mechanical ventilation at our hospital from April 2020 to May 2021. Plain chest X-rays were obtained and examined three times a week, and chest computed tomography (CT) images once a week on a routine schedule. During the first 48 hours after intratracheal intubation, a muscle relaxant was administered to suppress spontaneous breathing, and the peak inspiratory pressure (PIP) was controlled under 30 cmH_2O mainly by using the pressure control mode of the mechanical ventilator. A standard tidal volume (TV) setting and airway occlusion pressure ($P_{0.1}$) monitoring were used to minimize patient self-inflicted lung injury (P-SILI). Barotrauma, such as pneumothorax and/or pneumomediastinum, was diagnosed with the aid of plain X-ray or CT images. Details obtained from the medical records included demographics, onset episode, onset time, disposition, and mechanical ventilation settings ($P_{0.1}$, TV, PIP). The incidence and mortality of the patients with barotrauma were analyzed.

Results

Barotrauma occurred in 11 patients (8.5%) during the treatment for pneumonia: 5 had pneumothorax alone, 4 had pneumomediastinum alone, and 2 patients had both (Fig. 1). The average age of the patients who developed barotrauma was 73 years old. Most patients with pneumothorax had an onset episode of rapid SpO_2 decline, whereas patients with pneumomediastinum were diagnosed based on slow changes in plain X-ray images, worsening respiratory status, and the presence of subcutaneous emphysema. The average onset of barotrauma was 16 days after the onset of COVID-19 pneumonia and 7 days after tracheal intubation. All patients with pneumothorax were managed with tube thoracostomy. Eight patients died and 3 patients were transferred another hospital to continue treatment after the acute phase of pneumonia. The overall in-hospital mortality rate of the patients with severe COVID-19 pneumonia requiring mechanical ventilation was 23%, whereas that of the patients with barotrauma was 73%. After the onset of barotrauma, the average time to death was 16 days. Bronchial asthma was observed in 2 patients and diabetes mellitus in 1 patient. None had chronic obstructive pulmonary disease, and smoking history was unavailable

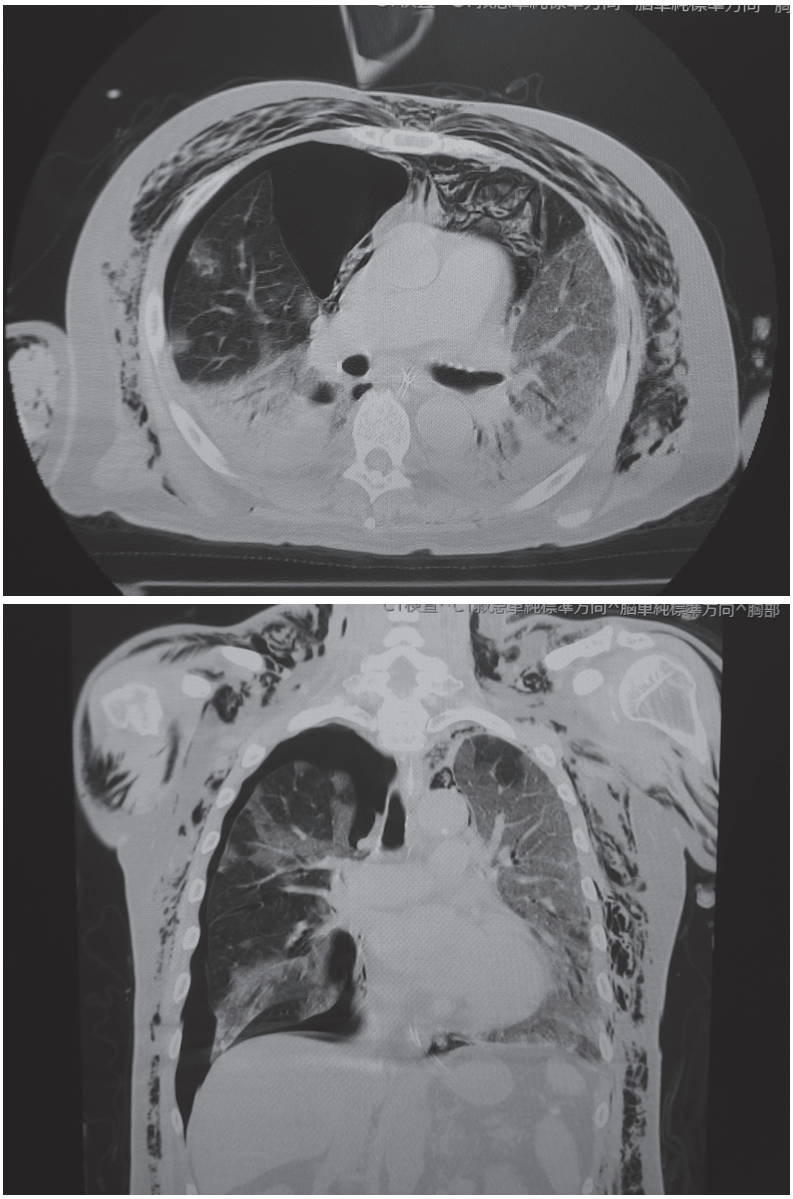

Figure 1. CT images of the 68-year-old male patient with pneumothorax and pneumomediastinum. Four days after tracheal intubation, his respiratory condition and subcutaneous emphysema worsened, and he died 6 days after the onset of barotrauma.

(Table 1).

During the treatment period, 43 of the 129 (33%) patients had a temporary peak inspiratory pressure exceeding 30 cmH_2O. In the patients with barotrauma, this rate was 43% before the occurrence of barotrauma. We investigated $P_{0.1}$, TV per standard body weight, and PIP during the 3 days before and after the onset date. The $P_{0.1}$ in all patients was less than 10 cmH_2O, but it exceeded 5 cmH_2O at some points (Fig. 2). This suggested that the patients with barotrauma were not controlled well enough to prevent P-SILI. No obvious change of $P_{0.1}$ was present before and after the onset of the barotrauma. TV tended to decrease after onset, whereas PIP was high before and after onset (Figs. 3 and 4). Taken together, these findings suggested that after the onset of barotrauma, it was still difficult to control the airway pressure even if the TV was set to the minimum.

Table 1. Characteristics of the patients with barotrauma

Patient	Age	Type of barotrauma	Onset episode	Days to onset after pneumonia	Days to onset after intubation	Days after onset	Discharge	Medical history	steroid dose
1	82	Pneumothorax	SpO_2, TV change	12	6	N/A	Death	Cerebral aneurysm	none
2	80	Pneumothorax	SpO_2 change after tracheostomy	18	14	5	Death	Asthma	dexamethasone 6.6mg 10days 3.3mg 7days
3	80	Pneumothorax	SpO_2 decline day after tracheostomy	23	13	N/A	Change hospital		mPSL 40mg 15days
4	87	Pneumothorax	Xp change, SpO_2 decline	12	5	25	Death	Diabetes, asthma	dexamethasone 6.6mg 10days 3.3mg 7days 1.65mg 8days
5	66	Pneumothorax	Xp change	25	6	13	Death		dexamethasone 6.6mg 10days 3.3mg 4days
6	64	Pneumomediastinum	Xp subcutaneous emphysema	24	13	30	Death		dexamethasone 6.6mg 16days
7	81	Pneumomediastinum	Xp subcutaneous emphysema	13	6	N/A	Change hospital	Angina	dexamethasone 6.6mg 10days 3.3mg 7days 1.65mg 7days
8	70	Pneumomediastinum	Xp subcutaneous emphysema	13	10	N/A	Change hospital	Hypertension	dexamethasone 6.6mg 10days
9	71	Pneumomediastinum	Xp subcutaneous emphysema	11	6	19	Death	Hypertension	dexamethasone 6.6mg 6days mPSL 1000mg 3days
10	56	Pneumothorax, pneumomediastinum	P/F decline, worsening of subcutaneous emphysema	13	1	13	Death		dexamethasone 6.6mg 10days
11	68	Pneumothorax, pneumomediastinum	Xp worsening of pneumothorax	20	4	6	Death	Dialysis, cerebral infarction	dexamethasone 6mg 13days 4mg 2days mPSL1000mg 3days

N/A, not available; P/F, partial pressure of arterial oxygen/fraction of inspired oxygen; SpO_2, oxygen saturation of peripheral artery; TV, tidal volume;and Xp, X-ray photo.

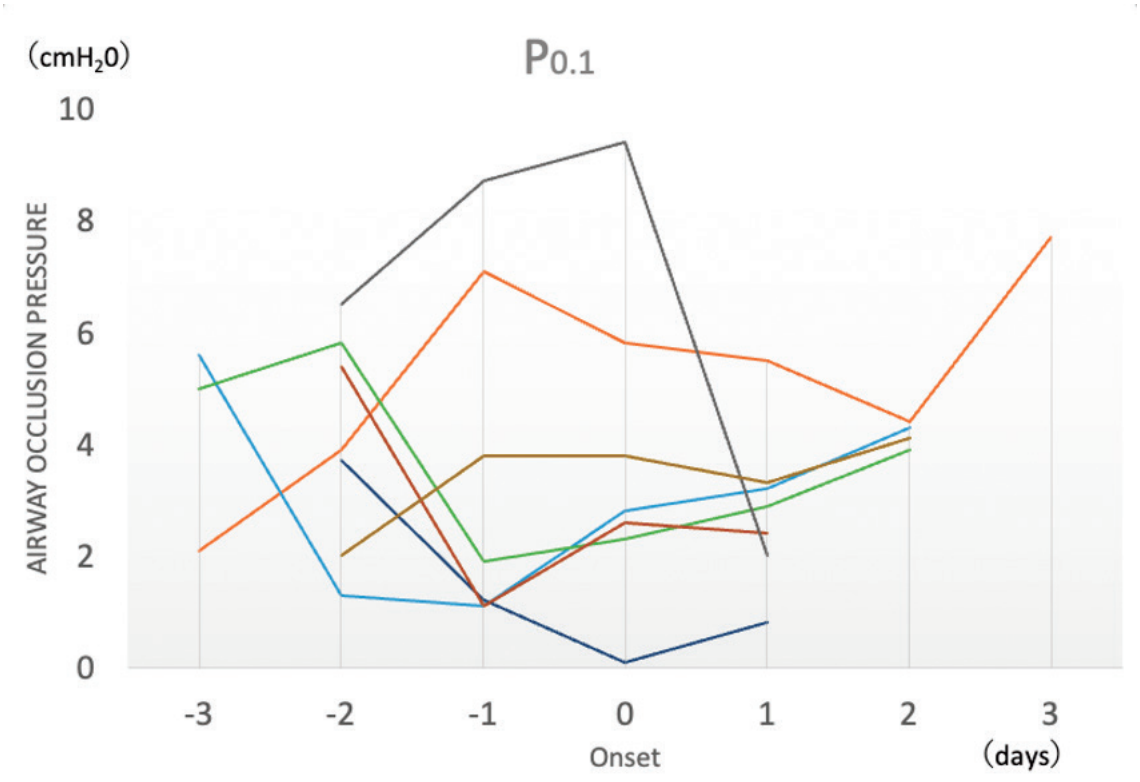

Figure 2. Airway occlusion pressures during the 7 days around the onset of barotrauma. Some pressures exceed 5 cmH_2O. No obvious changes are shown before and after onset.

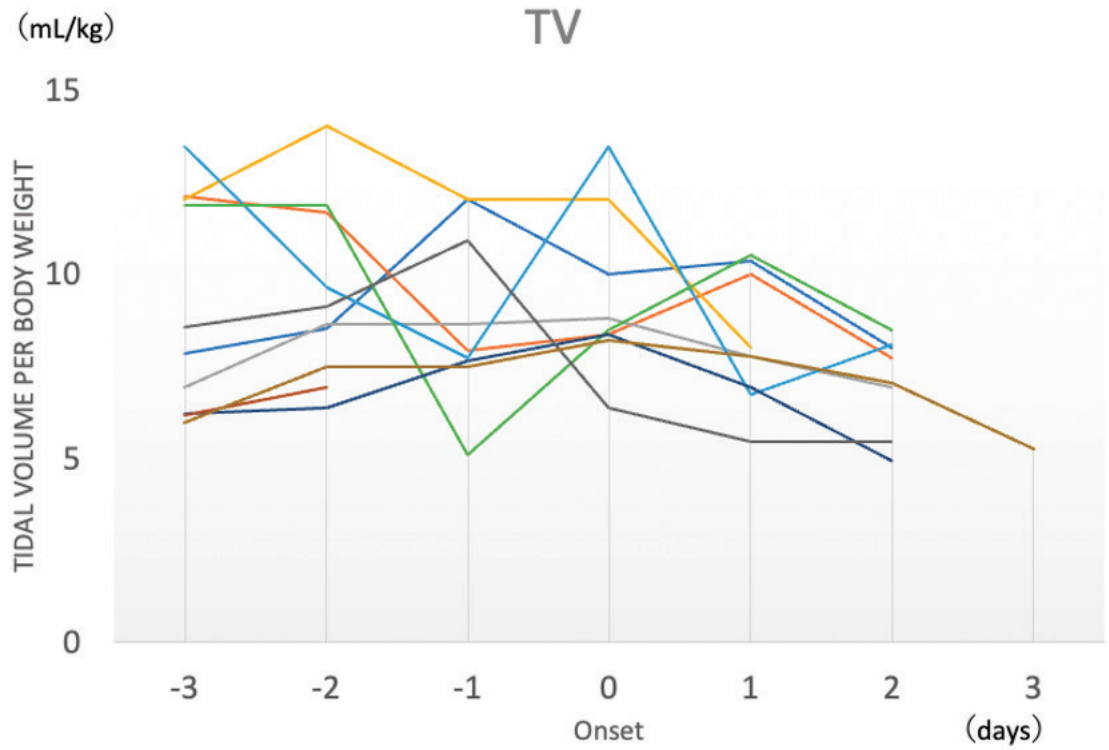

Figure 3. Tidal volume (TV) per standard body weight during the 7 days around the onset of barotrauma. TV tended to decrease after onset.

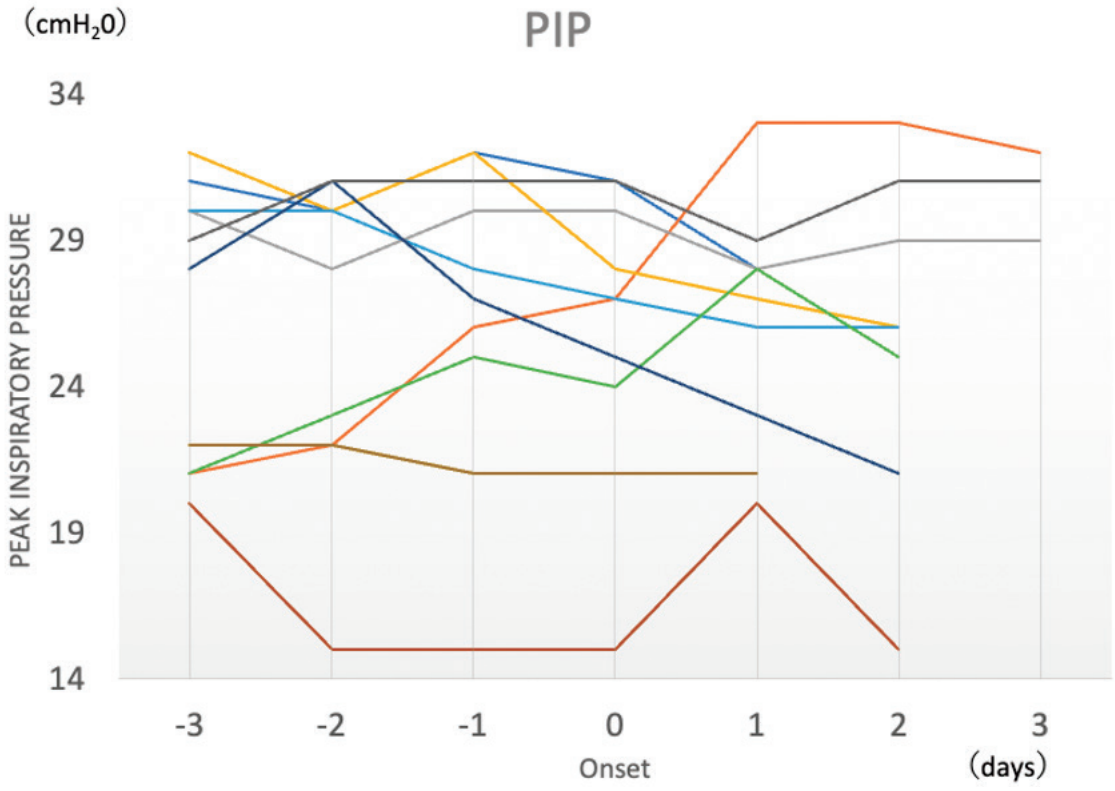

Figure 4. Peak inspiratory pressure (PIP) during the 7 days around the onset of barotrauma. PIP is high at all times around the onset date.

Discussion

In COVID-19 pneumonia, the virus triggers the immune system and induces the recruitment of inflammatory cells with subsequent production of pro-inflammatory cytokines and chemokines. This phenomenon results in interstitial and alveolar edema that leads to ARDS[1]. Although ARDS is managed with a high PEEP ventilator setting to prevent alveolar collapse, it is thought that the risk of alveolar damage increases due to the high peak pressure[2,3]. Severe and prolonged inflammation caused by the virus leads to the widespread destruction of alveoli and airspaces, increasing the likelihood of rupture with slight pressure changes from mechanical ventilation[4,5]. According to several reports, the incident of barotrauma is 2% in the patients with severe COVID-19 pneumonia and 10 to 40% in those undergoing mechanical ventilation[6-9]. S. Ozdemir et al reported that among the patients treated for COVID-19 pneumonia in the ICU, the incidence of pneumomediastinum was significantly higher in those treated with invasive mechanical ventilation than those treated with non-invasive mechanical ventilation[10]. The rate of barotrauma at our hospital was 8.5%, which is lower than that of previous reports, whereas the mortality rate of the patients with barotrauma was 73%, similar to that of other reports[11-14].

We set the TV as low as possible and airway peak pressure not to exceed 30 cmH_20, which is the same as the conventional ARDS treatment, to prevent ventilator-induced lung injury[15,16]. Furthermore, in recent years, the new concept of P-SILI has emerged, i.e., the possibility that lung injury is induced or worsened by the patient's own inspiratory effort. In particular, the more severe the lung injury is, the more frequently the trans-pulmonary pressure causes self-inflicted pulmonary injury. It has been reported that excessive pressure on the alveolar wall due to the patient's respiratory effort may induce inflammatory cells in the lungs and promote fibrosis[17-21]. At our hospital, muscle relaxant is administered for the first 48 hours after tracheal intubation, and $P_{0.1}$ is monitored to minimize P-SILI. If $P_{0.1}$ remains high after the decrease in muscle relaxation, the relaxant drug is continued for another 24 hours.

For respiratory management after barotrauma, we have no choice but to minimize TV to reduce the airway pressure, but PIP is still high, suggesting that barotrauma makes respiratory management even more difficult. In addition, $P_{0.1}$ was relatively high in the patients with barotrauma. We cannot determine whether this has an effect on the inability of patients with barotrauma to control P-SILI because there is no comparative data from patients without barotrauma.

The use of steroids for patients is recommended according to the treatment of ARDS, and most of the patients in this study also used steroids. Long-term steroid use has been implicated in alveolar destruction, and this effect is important[22-24]. However, there was a difference in the amount used, and some patients were given steroid pulses, but we thought that there was no definite trend (Table 1).

The treatment of COVID-19 pneumonia has changed significantly since the pandemic, due to viral mutation and the establishment of treatment methods. Even during the one-year period of this study, there were several changes of treatments for COVID-19 pneumonia in our institution, including the dose of steroids, antiviral drugs, and the timing of their use.

The limitations of this study are its small sample size, performance in a single facility, and lack of a cut-off value set for $P_{0.1}$. This study is just a case series study and there is no comparison data. Therefore, we cannot definitively state how relevant these treatments were to patient outcomes. It is undeniable that changes in treatment methods and strain mutations may have influenced this study.

Further study such as a large-scale comparative study is needed in the future.

In conclusion, the incidence of barotrauma in severe COVID-19 pneumonia at our hospital was low compared with that of previous reports. Precise management of mechanical ventilation with strict prevention of P-SILI might be one of the factors leading to this low incidence rate.

Acknowledgements

All authors have no COI to declare regarding the present study.

References

1. Batah SS, Fabro AT. Pulmonary pathology of ARDS in COVID19: a pathological review for clinicians. Respir Med 2021;176:106239.
2. Brower RG, Lanken PN, MacIntyre N, et al. Higher versus lower positive end-expiratory pressures in patients with the acute respiratory distress syndrome. N Engl J Med 2004;351:327-336.
3. Acute Respiratory Distress Syndrome Network; Brower RG, Matthay MA, et al. Ventilation with lower tidal volumes as compared with traditional tidal volumes for acute lung injury and the acute respiratory distress syndrome. N Engl J Med 2000;342:1301-1308.
4. Ferreira JG, Rapparini C, Gomes BM, et al. Pneumothorax as a late complication of COVID-19. Rev Inst Med Trop Sao Paulo 2020;62:e61.
5. Sun R, Liu H, Wang X. Mediastinal emphysema, giant bulla, and pneumothorax developed during the course of COVID-19 pneumonia. Korean J Radiol 2020;21:541-544.
6. Lemmers DHL, Hilal MA, Bnà C, et al. Pneumomediastinum and subcutaneous emphysema in COVID-19: barotrauma or lung frailty? ERJ Open Res 2020;6:00385-02020.
7. Edwards JA, Breitman I, Bienstock J, et al. Pulmonary barotrauma in mechanically ventilated coronavirus disease 2019 patients: a case series. Ann Med Surg (Lond) 2020;61:24-29.
8. Martinelli AW, Ingle T, Newman J, et al. COVID-19 and pneumothorax: a multicentre retrospective case series. Eur Respir J 2020;56:2002697.
9. Capaccione KM, D'souza B, Leb J, et al. Pneumothorax rate in intubated patients with COVID-19. Acute Crit Care 2021;36:81-84.
10. Özdemir S, Bilgi DÖ, Hergünsel GO, et al. Incidence and risk factors for pneumomediastinum in COVID-19 patients in the intensive care unit. Interact Cardiovasc Thorac Surg. 2022;34:236-244.
11. Elsaaran H, AlQinai S, AlTarrah D, et al. Prevalence and risk factors of barotrauma in Covid-19 patients admitted to an intensive care unit in Kuwait; a retrospective cohort study. Ann Med Surg (Lond) 2021;63: 102141.
12. Chilimuri S, Sun H, Alemam A, et al. Predictors of mortality in adults admitted with COVID-19: retrospective cohort study from New York City. West J Emerg Med 2020;21:779-784.
13. Imam Z, Odish F, Gill I, et al. Older age and comorbidity are independent mortality predictors in a large cohort of 1305 COVID-19 patients in Michigan, United States. J Intern Med 2020;288:469-476.
14. Palaiodimos L, Kokkinidis DG, Li W, et al. Severe obesity, increasing age and male sex are independently associated with worse in-hospital outcomes, and higher in-hospital mortality, in a cohort of patients with COVID-19 in the Bronx, New York. Metabolism 2020;108:154262.
15. Gattinoni L, Tonetti T, Cressoni M, et al. Ventilator-related causes of lung injury: the mechanical power. Intensive Care Med 2016;42:1567-1575.
16. Hraiech S, Dizier S, Papazian L. The use of paralytics in patients with acute respiratory distress syndrome. Clin Chest Med 2014;35:753-763.
17. Grieco DL, Menga LS, Eleuteri D, et al. Patient self-inflicted lung injury: implications for acute hypoxemic respiratory failure and ARDS patients on non-invasive support. Minerva Anestesiol 2019;85:1014-1023.
18. Carteaux G, Parfait M, Combet M, et al. Patient-self inflicted lung injury: a practical review. J Clin Med 2021; 10:2738.
19. Yoshida T, Grieco DL, Brochard L, et al. Patient self-inflicted lung injury and positive end-expiratory pressure for safe spontaneous breathing. Curr Opin Crit Care 2020;26:59-65.
20. Battaglini D, Robba C, Ball L, et al. Noninvasive respiratory support and patient self-inflicted lung injury in COVID-19: a narrative review. Br J Anaesth 2021;127:353-364.
21. Neetz B, Flohr T, Herth FJF, et al. Patient self-inflicted lung injury (P-SILI): from pathophysiology to clinical evaluation with differentiated management. Med Klin Intensivmed Notfmed 2021;116:614-623. (In German)
22. van Schaik E, Ramnarain D, Pouwels S. Pneumothorax due to a nontraumatic thoracic wall rupture due to

steroid-induced muscle wasting. Ann Thorac Surg. 2021;112:e237-e239.
23. Kadota T, Shimizu K, Tsurushige C, et al. Organizing pneumonia complicated by cyst and pneumothorax formation. Intern Med. 2012;51:3155-3158.
24. Yamaya T, Baba T, Hagiwara E, et al. Pneumothorax in a COVID-19 Pneumonia patient without underlying risk factors. Intern Med. 2020;59:2921-2925.

Osaka City Med. J. Vol. 69, 75-82, 2023

A Case of Conversion Surgery for Pancreatic Head Cancer with Liver Metastases and Renal Anemia after Combination Therapy with Anticancer Agents and a Hypoxia-inducible Factor Prolyl Hydroxylase Inhibitor

Go Ohira[1)], Ryosuke Amano[1)], Shogo Tanaka[1)], Kenjiro Kimura[1)], Hiroji Shinkawa[1)], Kohei Nishio[1)], Masahiko Kinoshita[1)], Jun Tauchi[1)], Daisuke Shirai[2)], Takuma Okada[2)], Takahito Kawaguchi[1)], Naoki Tani[2)], and Takeaki Ishizawa[1)]

Department of Hepatobiliary-Pancreatic Surgery[1)], Graduate School of Medicine, Osaka Metropolitan University ; and
Department of Hepatobiliary-Pancreatic Surgery[2)], Graduate School of Medicine, Osaka City University

Abstract

This report describes a case of conversion surgery for pancreatic head cancer with liver metastases and renal anemia after combination therapy with anticancer agents and a hypoxia-inducible factor prolyl hydroxylase inhibitor.

A 70-year-old woman who visited the urology department for follow-up of postoperative bladder cancer and chronic renal failure was diagnosed with pancreatic head cancer. Computed tomography and magnetic resonance imaging revealed no evidence of distant metastasis, and surgery was performed. Two nodules approximately 10 mm in size were found on the liver surface and removed. The nodules were diagnosed as metastases by rapid examination. Chemotherapy was started 4 days after surgery. During outpatient chemotherapy, progression of renal anemia was observed, and transfusion and erythropoietin injection were performed once, followed by Vadadustat, which made it possible to continue chemotherapy on an outpatient basis without transfusions or erythropoietin injections. Conversion surgery was performed 17 months after the initial diagnosis without the appearance of distant metastasis. The patient has been under observation after conversion surgery without recurrence for approximately 7 months.

Vadadustat was safely used in a patient with pancreatic cancer and renal dysfunction, and it effectively improved renal anemia, allowing the patient to continue outpatient chemotherapy.

Key Words: Pancreatic adenocarcinoma; Conversion surgery; Renal anemia; Hypoxia-inducible factor prolyl hydroxylase inhibitor; Liver metastasis

Received January 5, 2023; accepted June 13, 2023.
Correspondence to: Takeaki Ishizawa, MD, PhD, FACS.
Department of Hepatobiliary-Pancreatic Surgery, Graduate School of Medicine, Osaka Metropolitan University, 1-4-3 Asahimachi, Abeno-ku, Osaka 545-8585, Japan
Tel: +81-6-6645-3840; Fax: +81-6-6646-6057
E-mail: take1438@gmail.com

Introduction

Recently, an increasing number of prospective studies including randomized controlled studies have described the efficacy of preoperative chemotherapy for pancreatic adenocarcinoma[1-3]. In clinical situations, it is often difficult to continue the administration of effective doses of anticancer agents for patients with renal failure, especially in the presence of refractory anemia.

A hypoxia-inducible factor prolyl hydroxylase inhibitor (HIP-PHI) is a hypoxia-inducible factor (HIF), a regulator of red blood cell production in the body, which increases the production of erythropoietin (EPO). It also induces the expression of various genes involved in iron metabolism and suppresses hepcidin to increase iron utilization efficiency, thereby improving anemia[4-6].

In this study, we report a case of pancreatic head cancer with liver metastases and chronic renal failure associated with severe anemia that was treated by conversion pancreaticoduodenectomy after chemotherapy (gemcitabine plus nanoparticle albumin-bound paclitaxel [GnP]) in combination with a HIF-PHI.

Case report

In 2020, a 70-year-old woman was referred to our department from the urology department because pancreatic head cancer was suggested by plain computed tomography (CT) (Fig. 1A) during follow-up for postoperative bladder cancer and chronic renal failure. Endoscopic ultrasound-guided fine needle aspiration disclosed an adenocarcinoma lesion 20 mm in diameter in the pancreatic head (Fig. 1B). Because no vascular invasion or distant metastasis was identified by preoperative imaging studies including magnetic resonance imaging (MRI), the patient first underwent surgery with curative intent. At laparotomy, two nodules approximately 10 mm in size were found on hepatic surfaces (Fig. 2), which were identified as metastatic adenocarcinoma by intraoperative rapid diagnosis. Therefore, the surgery was completed with removal of only two nodules of the liver, and chemotherapy was considered. The Union for international cancer control (UICC) TNM 8th edition classification at this point was T2N0M1 Stage Ⅳ[7].

Because of the patient's poor renal function (serum blood urea nitrogen [BUN], 41 mg/dL; creatinine [Cre]), 2.6 mg/dL; estimated glomerular filtration rate [eGFR]), 14.89 mL/min/1.7m^2), GnP was selected as the anticancer regimen. At the same time, the patient had macrocytic anemia (red blood cell, 214×10^4/μL; hemoglobin [Hb], 7.0 g/dL; hematocrit, 21.7%; mean corpuscular volume, 101 fL; mean corpscular hemoglobin, 32.7 pg; mean corpuscular hemoglobin consentration, 32.3% and reticulocyte count, 13.5%) that was diagnosed as renal anemia because of the lack of findings suggesting folate/vitamin B12 deficiency (folic acid, 5.4 ng/mL; vitamin B12, 642 pg/mL) or defective iron utilization (Fe, 20 μg/dL, total iron binding capacity, 188 μg/dL and ferritin, 348 ng/mL). Initially, GnP (normal regimen : gemcitabine, 1000 mg/BSA; nab-paclitaxel, 125 mg/BSA administered on days 1, 8, and 15, every 28 days.) had been administered at 80% of the usual dose on biweekly in combination with transfusion and EPO injection. However, renal anemia became refractory to the conventional treatment, making it difficult to continue GnP therapy on an outpatient basis after three courses despite the rapid response in terms of tumor markers such as colorectal carcinoma antigen 19-9 (CA19-9) and s-pancreas-1 (SPan-1)[8] (Fig. 3). Therefore, we decided to administer an HIF-PHI (vadadustat, Vafseo®, Mitsubishi Tanabe Pharma Corporation, Osaka, Japan; oral 300 mg/day) in an attempt to improve anemic conditions through the production of intrinsic erythropoietin and improvement of iron utilization[9]. Vadadustat prescribed one tablet a day while checking blood

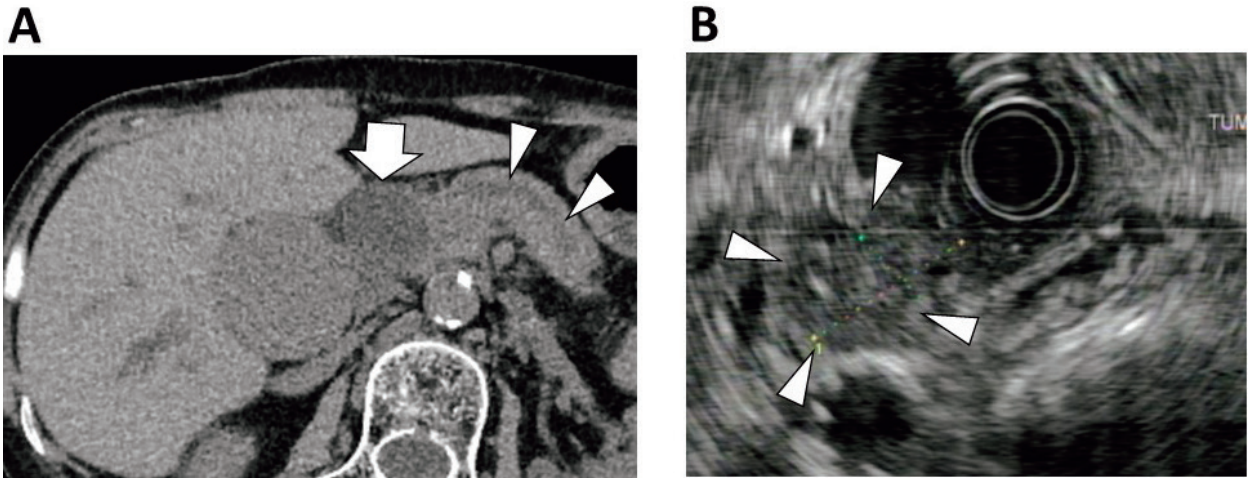

Figure 1. Imaging studies.
A: Plain computed tomography before the initial surgery revealed dilatation of the main pancreatic duct (arrowheads) and common bile duct (arrow), although the boundaries of the pancreatic tumor were unclear. No distant metastases were suggested.
B: Endoscopic ultrasound before the initial surgery revealed a 20-mm hypoechoic nodule in the pancreatic head (arrowheads). Fine needle aspiration confirmed the presence of adenocarcinoma.

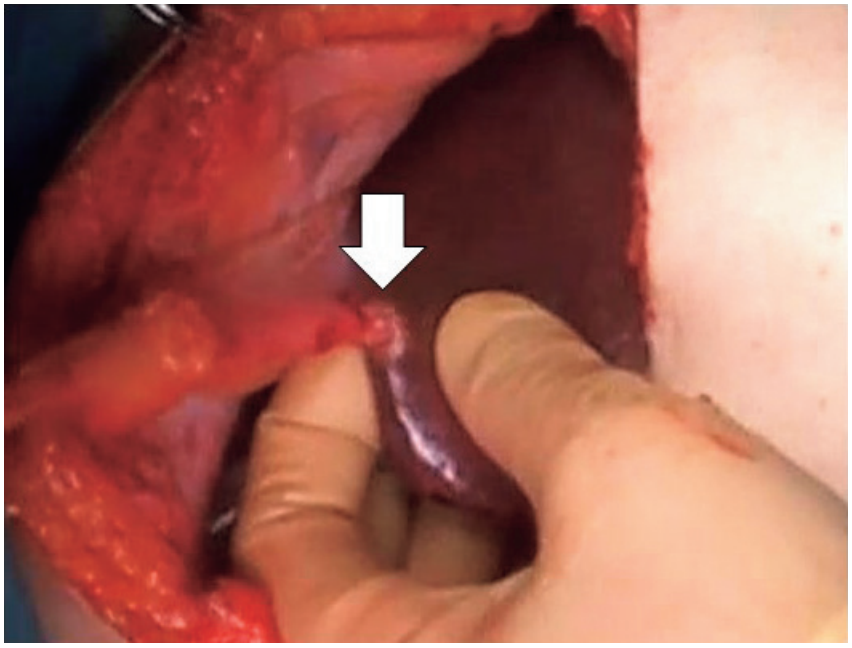

Figure 2. Liver metastases found in the initial surgery.
A yellowish-white nodule approximately 10 mm in diameter was observed on the surface of hepatic S3 beside the round ligament (arrow). Another tumor in hepatic S2 (8 mm in diameter) was confirmed only by palpation and ultrasound.

samples every two weeks to keep it to the minimum necessary. Consequently, anemia was controlled in the Hb range of 8-9 g/dL, enabling the continuation of GnP therapy after reducing the dose by 50% and on triweekly. 14 courses of GnP (a total of 22 infusions with 6 discontinuations) were performed. Side effects of GnP were mild hair loss and peripheral neuropathy of limbs, but chemotherapy could be continued. Vadadustat had no noticeable side effects than mild nausea.

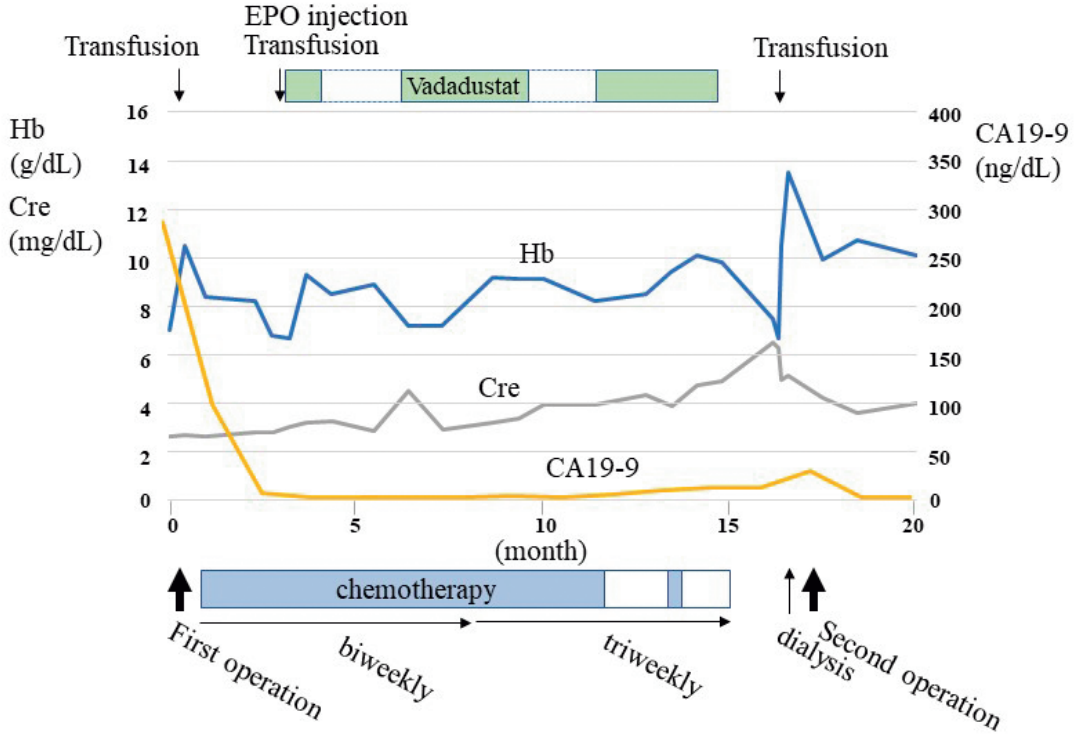

Figure 3. Therapeutic course of chemotherapy and the status of renal function/anemia between the two surgeries.
A hypoxia-inducible factor prolyl hydroxylase inhibitor was first administered 2 months after the start of chemotherapy targeting Hb levels of 8-9 g/dL. In total, 12 courses of gemcitabine plus nanoparticle albumin-bound paclitaxel (GnP) had been indicated, but the dose was reduced by 50% because of the gradual deterioration of renal function. Tumor marker (CA19-9) levels rapidly decreased immediately after the start of GnP therapy and remained in normal ranges until curative resection.

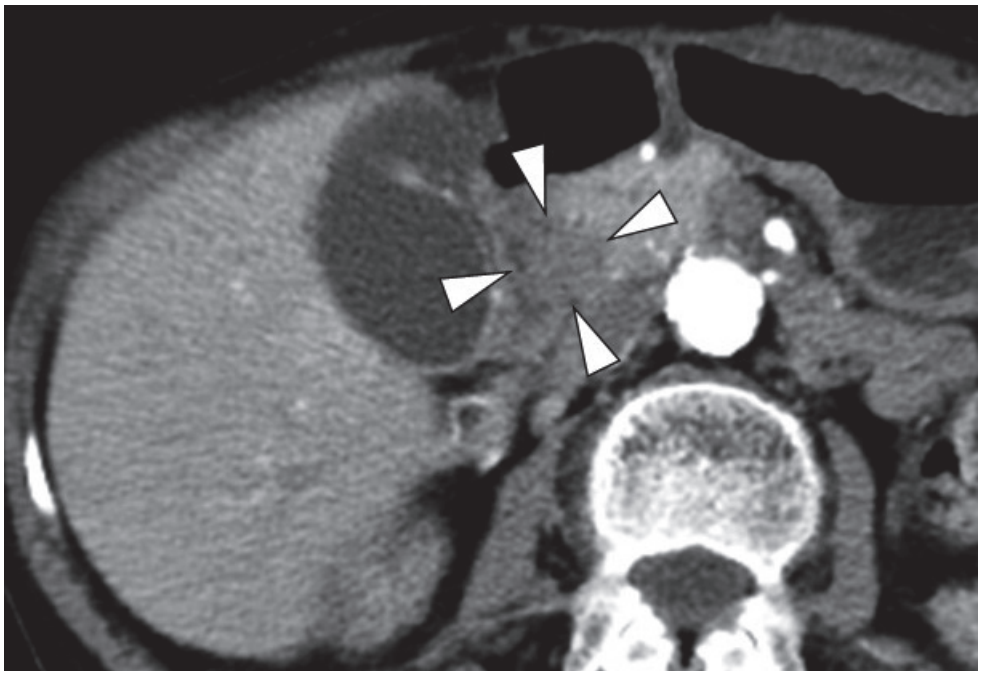

Figure 4. Imaging studies.
Contrast-enhanced computed tomography after chemotherapy revealed a 20-mm hypovascular tumor in the pancreatic head (arrowheads). The dilatation of the main pancreatic duct and common bile duct identified before chemotherapy was relieved. No metastatic lesions were demonstrated.

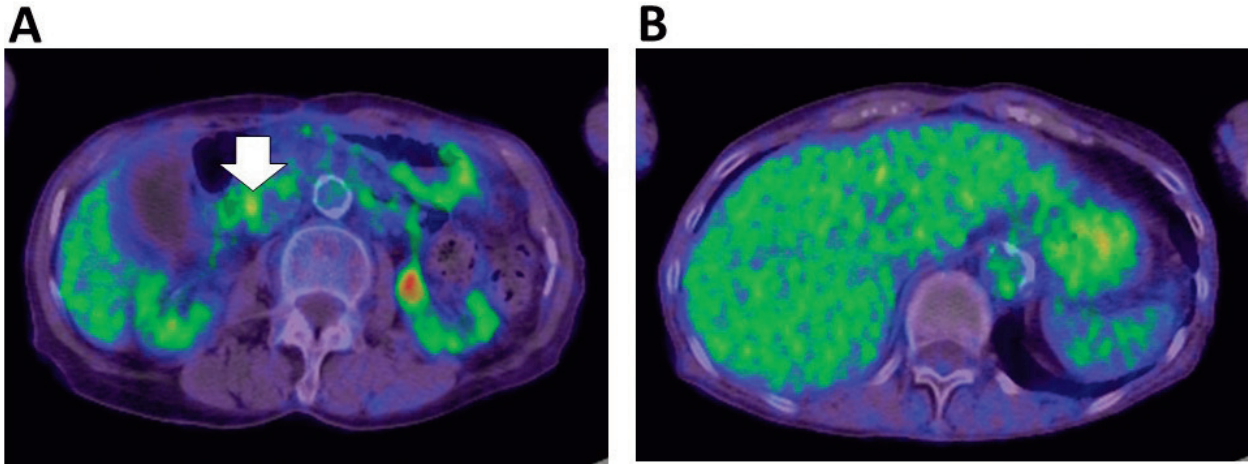

Figure 5. Imaging studies.
A: Positron emission tomography revealed slight accumulation (SUVmax=5) in the pancreatic head lesion (arrow). B: No metastatic signals were visualized in the liver .

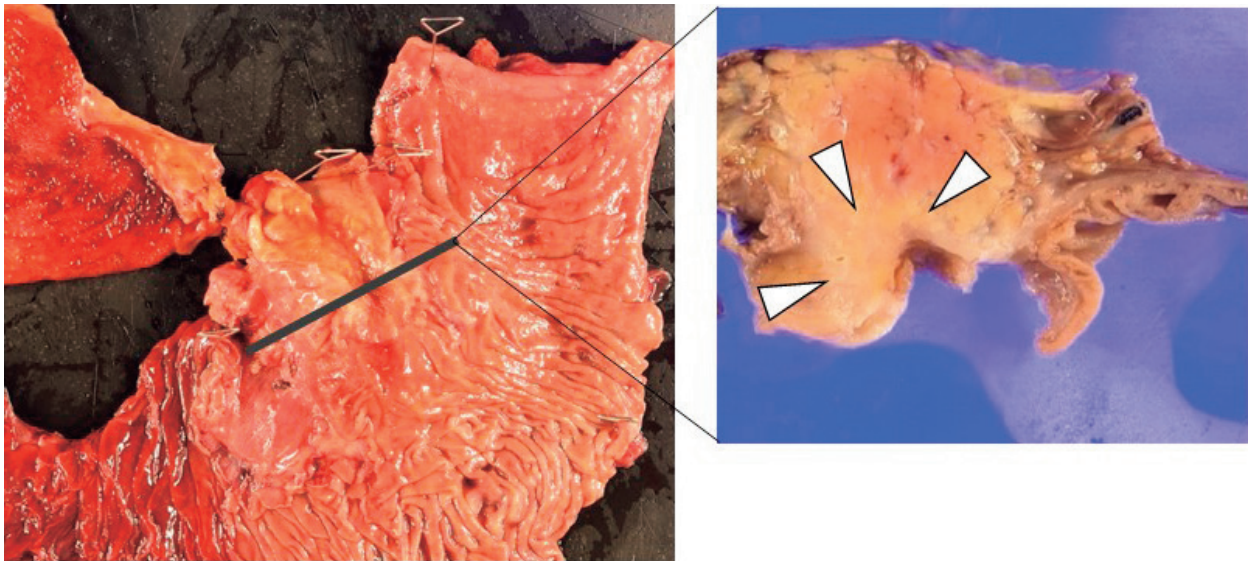

Figure 6. Histopathological images.
About 15 mm of cancer remained around the bile duct, and infiltration was observed (arrow).

Fifteen months after first operation, imaging studies including contrast-enhanced CT (Fig. 4), MRI, and positron-emission tomography revealed no viable lesions excluding the shrunken (15 mm in diameter) primary tumor in the pancreatic head (Fig. 5). Tumor marker levels remained within normal ranges. By contrast, the patient's renal dysfunction gradually progressed (serum Cre, 4.87 mg/dL; eGFR, 7.43 mL/min/1.7m^2), making it impossible to undergo further chemotherapy. Then, we offered conversion pancreaticoduodenectomy with adjustment of acidosis with continuous hemodiafiltration.

In the second surgery, no surgical contraindications such as liver metastases and peritoneal disseminations were found, and pancreaticoduodenectomy was completed in the usual manner. The operative time and estimated blood loss were 378 min and 300 mL, respectively. The postoperative course was uneventful, although hospitalization was prolonged because a shunt was created for future hemodialysis. The pathological diagnosis of the resected specimen was Ph, mod, pT3, int,

INFb, ly0, v0, ne1, mpdx, pCH1, pDU0, pS0, pRP0, pPV0, pA0, pPL0, pOO0, pPCM0, pBCM0, pDPM0; Evans grade Ⅲ (Fig. 6)[10]. Currently, the patient is alive with no evidence of recurrence 7 months after the conversion surgery (24 months after the initial diagnosis).

Discussion

Despite recent evidence suggesting the efficacy of preoperative chemotherapy for pancreatic adenocarcinoma, the optimal regimens for patients with renal dysfunction remain unclear. In our department, GnP has usually been selected as a chemotherapeutic regimen in patients with renal failure based on the fact that gemcitabine is degraded in blood to uracil metabolites, which are not toxic to the kidneys[11,12], and paclitaxel is mainly excreted into bile. In this patient, the introduction of an HIF-PHI in place of transfusion and EPO injections played a key role in assuring the safety and feasibility of chemotherapy on an outpatient basis . This strategy enabled 12 courses of GnP therapy, controlling the primary cancer and possible metastatic lesions for 15 months after exploratory laparotomy.

An HIF-PHI was first delivered to clinical practices in Japan in November 2019 as a therapeutic drug for renal anemia during hemodialysis and then extended to patients with chronic renal failure in 2020. Vadadustat improves renal anemia by enhancing endogenous erythropoietin production through the stabilization of HIFα enabled by its inhibitory effect on HIF prolyl hydroxylase as well as improving iron metabolism[13,14]. In addition to its pharmaceutical mechanism of action, oral vadadustat has potential advantages over EPO injections in terms of feasibility, especially in outpatients requiring frequent infusion treatments such as chemotherapy for malignant diseases. In fact, some authors have suggested the efficacy of HIF-PHIs in the treatment of renal anemia during chemotherapy for renal cancer[15].

Potential concerns about the use of HIP-PHI therapy during chemotherapy include the activation of vascular endothelial growth factor, which can enhance tumor angiogenesis. In animal studies, trends of increased rates of mammary gland tumors and lung tumors were revealed, although these events occurred following the use of an HIP-PHI at a 143-fold higher dose than the clinical dose[16]. Conversely, other groups reported the inhibition of cancer progression by HIF-PHI therapy in mice, probably because of the improvements of blood flow and the oxygen distribution in cancerous tissues because of the normalization of blood vessels[17]. In this patient, we planned to administer a minimal dose of an HIF-PHI to achieve Hb levels of 8-9 g/dL, aiming to avoid the potential risk of tumor progression during chemotherapy. Other possible risks of HIF-PHI therapy in patients with cancer undergoing curative surgery include the aggravation of diabetic retinopathy, liver dysfunction, and development of thromboembolic diseases[9].

Despite recent advances in surgical techniques and chemotherapy, the survival benefit of conversion surgery for pancreatic cancer with distant metastasis remains controversial. In previous series of pancreatic cancer with liver metastases, favorable long-term outcomes were recorded (median overall survival, 18.2-34 months)[18-22] after curative resection under conditions in which the primary cancer and distant lesions could be controlled by chemotherapy for at least 8 months[23-25]. This patient decided to undergo curative resection because the deterioration of renal function made it difficult to continue effective chemotherapy after 15 months of disease control. Although she has remained alive without evidence of recurrence for 7 months after the conversion surgery, we must follow-up this patient for years to evaluate the oncological benefit of our strategy consisting of GnP

therapy in combination with HIF-PHI therapy for refractory renal anemia.

Acknowledgement

All authors have no COI to declare regarding the present study. We have obtained the informed consent for this case report.

We thank Joe Barber Jr., PhD, from Edanz (https://www.jp.edanz.com/ac), for editing a draft of this manuscript.

References

1. Motoi F, Kosuge T, Ueno H, et al. Randomized phase Ⅱ/Ⅲ trial of neoadjuvant chemotherapy with gemcitabine and S-1 versus upfront surgery for resectable pancreatic cancer (Prep-02/JSAP-05). Jpn J Clin Oncol 2019;49: 190-194.
2. Birrer DL, Golcher H, Casadei R, et al. Neoadjuvant therapy for resectable pancreatic cancer: a new standard of care. pooled data from 3 randomized controlled trials. Ann Surg. 2021;274:713-720.
3. Casadei R, Di Marco M, Ricci C, et al. Neoadjuvant chemoradiotherapy and surgery versus surgery alone in resectable pancreatic cancer: a single-center prospective, randomized, controlled trial which failed to achieve accrual targets. J Gastrointest Surg 2015;19:1802-1812.
4. Maxwell PH, Eckartdt KU. HIF prolyl hydroxylase inhibitors for the treatment of renal anaemia and beyond. Nat Rev Nephrol 2016;12:157-168.
5. Koury MJ, Haase VH. Anaemia in kidney disease: harnessing hypoxia responses for therapy. Nat Rev Nephrol 2015;11:394-410.
6. Gupta N, Wish JB. Hypoxia-inducible factor prolyl hydroxylase inhibitors: a potential new treatment for anemia in patients with CKD. Am J Kidney Dis 2017;69:815-826.
7. Brierley J.D, Gospodarowicz M.K, Wittekind C, et al. editors. TNM Classification of Malignant Tumours. 8th ed. Wiley-Blackwell: 2016. pp. 93.
8. Chung YS, Ho JJ, Kim YS, et al. The detection of human pancreatic cancer-associated antigen in the serum of cancer patients. Cancer 1987;60:1636-1643.
9. Eckardt KU, Agarwal R, Aswad A, et al. Safety and efficacy of vadadustat for anemia in patients undergoing dialysis. N Engl J Med 2021;384:1601-1612.
10. Evans DB, Rich TA, Byrd DR, et al. Preoperative chemoradiation and pancreaticoduodenectomy for adenocarcinoma of the pancreas. Arch Surg 1992;127:1335-1339.
11. Masumori N, Kunishima Y, Hirobe M, et al. Measurement of plasma concentration of gemcitabine and its metabolite dF-dU in hemodialysis patients with advanced urothelial cancer. Jpn J Clin Oncol 2008;38:182-185.
12. Tomimaru Y, Eguchi H, Satoh T, et al. Feasibility of pre-operative chemoradiotherapy with gemcitabine to treat pancreatic cancer in patients with impaired renal function. Jpn J Clin Oncol 2015;45:343-348.
13. Stockmann C, Fandrey J. Hypoxia-induced erythropoietin production: a paradigm for oxygen-regulated gene expression. Clin Exp Pharmacol Physiol 2006;33:968-979.
14. Yeo EJ, Cho YS, Kim MS, et al. Contribution of HIF-1alpha or HIF-2alpha to erythropoietin expression: in vivo evidence based on chromatin immunoprecipitation. Ann Hematol 2008;87:11-17.
15. Zhou QQ, Li J, Liu B, et al. Roxadustat for treatment of anemia in a cancer patient with end-stage renal disease: a case report. World J Clin Cases 2022;10:6587-6594.
16. Adams DF, Watkins MS, Durette L, et al. Carcinogenicity assessment of daprodustat (GSK1278863), a hypoxia-inducible factor (HIF)-prolyl hydroxylase inhibitor. Toxicol Pathol 2020;48:362-378.
17. Nishide S, Matsunaga S, Shiota M, et al. Controlling the phenotype of tumor-infiltrating macrophages via the PHD-HIF axis inhibits tumor growth in a mouse model. iScience 2019;19:940-954.
18. Sakaguchi T, Valente R, Tanaka K, et al. Surgical treatment of metastatic pancreatic ductal adenocarcinoma: a review of current literature. Pancreatology 2019;19:672-680.
19. Frigerio I, Regi P, Giardino A, et al. Downstaging in stage Ⅳ pancreatic cancer: a new population eligible for surgery? Ann Surg Oncol 2017;24:2397-2403.
20. Wright GP, Poruk KE, Zenati MS, et al. Primary tumor resection following favorable response to systemic chemotherapy in stage Ⅳ pancreatic adenocarcinoma with synchronous metastases: a bi-institutional analysis. J Gastrointest Surg 2016;20:1830-1835.
21. Schneitler S, Kröpil P, Riemer J, et al. Metastasized pancreatic carcinoma with neoadjuvant FOLFIRINOX therapy and R0 resection. World J Gastroenterol 2015;21:6384-6390.

22. Shimura M, Mizuma M, Hayashi H, et al. A long-term survival case treated with conversion surgery following chemotherapy after diagnostic metastasectomy for pancreatic cancer with synchronous liver metastasis. Surg Case Rep 2017;3:132.
23. Lemke J, Barth TF, Juchems M, et al. Long-term survival following resection of brain metastases from pancreatic cancer. Anticancer Res 2011;31:4599-4603.
24. Ushida Y, Inoue Y, Oba A, et al. Optimizing indications for conversion surgery based on analysis of 454 consecutive Japanese cases with unresectable pancreatic cancer who received modified FOLFIRINOX or gemcitabine plus nab-paclitaxel: a single-center retrospective study. Ann Surg Oncol 2022;29:5038-5050.
25. Satoi S, Yamaue H, Kato K, et al. Role of adjuvant surgery for patients with initially unresectable pancreatic cancer with a long-term favorable response to non-surgical anti-cancer treatments: results of a project study for pancreatic surgery by the Japanese Society of Hepato-Biliary-Pancreatic Surgery. J Hepatobiliary Pancreat Sci 2013;20:590-600.

Osaka City Med. J. Vol. 69, 83-88, 2023

Domino Reconstruction of a Mycotic Aneurysm in the Common Iliac Artery Using an Autologous Graft from the Contralateral Iliac Artery

Akihiro Sumiya[1], Yasuyuki Bito[1], Takanobu Aoyama[1], Masanori Sakaguchi[1], Yuriko Kiriya[2], and Takashi Murakami[1]

Department of Cardiovascular Surgery[1], Osaka City General Hospital; and Department of Cardiovascular Surgery[2], Lampang Hospital

Abstract

85-year-old male patient presented with a mycotic aneurysm in the right common iliac artery. The left iliac artery was harvested beforehand and replaced with expanded polytetrafluoroethylene graft. The mycotic aneurysm was subsequently dissected and reconstruction was performed using autologous left iliac artery. A bypass was placed from the left external iliac artery to the right deep femoral artery because both the right external iliac artery and right superficial femoral artery was originally occluded. This domino reconstruction provided an autologous arterial graft for the infected lesion, which was supposed to be more resistant to infection than any other synthetic materials.

Key Words: Domino reconstruction; Autologous iliac artery graft; Mycotic aneurysm

Introduction

A mycotic aneurysm remains a serious condition that is associated with high morbidity and mortality[1]. An optimal treatment strategy, including the most appropriate surgical technique and material, has been discussed. Here, we report the case of a patient who presented with a mycotic aneurysm in the common iliac artery and was successfully treated by debridement and domino reconstruction using the autologous contralateral external iliac artery and expanded polytetrafluoroethylene (ePTFE) grafts. The patient provided consent for the writing, publication, and display of photographs in this case report.

Case Report

An 85-year-old male patient was admitted to our division for the surgical treatment of a mycotic aneurysm in the iliac artery. A follow-up computed tomography (CT) scan for bladder cancer revealed a rapidly growing saccular aneurysm in the right common iliac artery with an irregular contour, leading to the diagnosis of a mycotic aneurysm (Figs. 1A and 1B). A blood culture was negative for pathogens. Obstruction of the right external iliac artery (EIA) and superficial femoral artery was also

Received January 17, 2023; accepted June 13, 2023.
Correspondence to: Akihiro Sumiya, MD.
Department of Cardiovascular Surgery, Osaka City General Hospital,
2-13-22 Miyakojimahondori, Miyakojima-ku, Osaka 534-0021, Japan.
Tel: +81-6-6929-1221; Fax: +81-6-6929-3273
E-mail: aki.0809.ocum@gmail.com

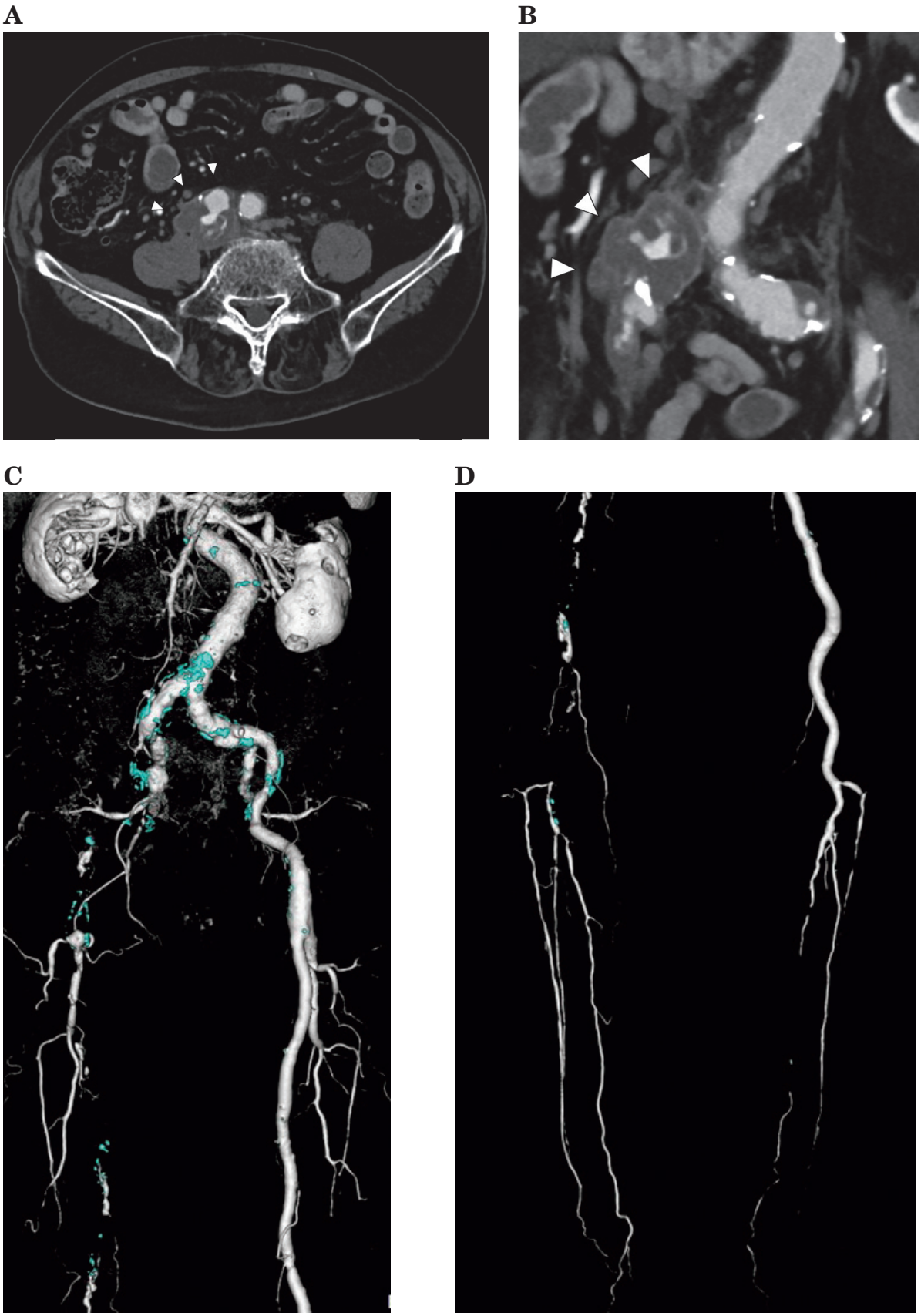

Figure 1. Preoperative computed tomographic angiogram. A saccular aneurysm with an irregular contour (arrow heads) is seen in the right common iliac artery. (**A**: axial, **B**: coronal) **C**, **D**: The right external iliac artery and superficial femoral artery are obstructed.

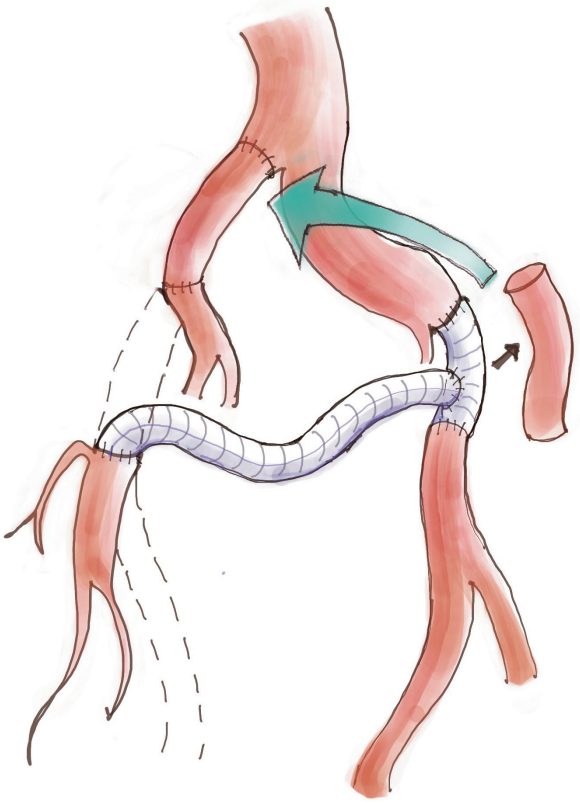

Figure 2. Schematic drawing of the surgery.

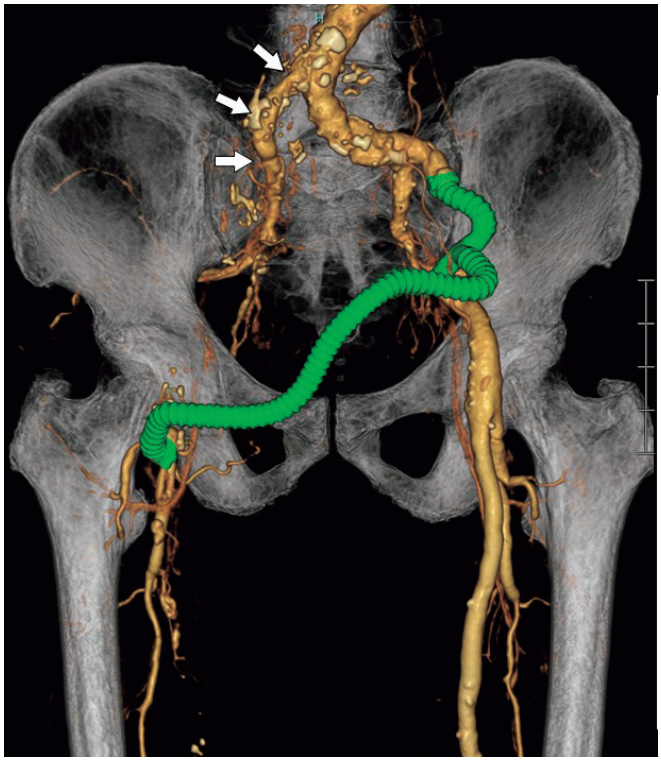

Figure 3. Computed tomographic angiogram after the surgery revealing patent autologous iliac artery (arrows) and expanded polytetrafluoroethylene (ePTFE) grafts (green). The prosthesis graft was used for replacement of the left external iliac artery, and the graft-to-deep femoral artery bypass was used to treat ischemia in the right extremity ischemia.

observed (Figs. 1C and 1D).

Prior to surgically accessing the infected lesion, a contralateral para-rectal incision was made, and an autologous graft from the left EIA was harvested via an extraperitoneal approach and replaced with an 8-mm ePTFE graft (GORE® PROPATEN® Vascular Graft; W.L. Gore & Associates, Inc., Flagstaff, AZ, USA). An additional extra-anatomical bypass from the graft-to-right deep femoral artery was constructed to treat the occluded right EIA (Fig. 2). Both grafts were placed in clean fields, and the resulting wounds were closed before the next surgical step to prevent contamination. A median laparotomy was subsequently performed, and intravenous heparin was administered prior to clamping the terminal aorta and left common iliac artery. The mycotic aneurysmal sac was opened, and the right internal iliac artery (ⅡA) was clamped using an 8 Fr balloon catheter. The aneurysm was debrided, and the resulting tissue was sent to the pathology laboratory for culture. Domino reconstruction from the terminal aorta to the right ⅡA was completed with the previously harvested autologous graft.

The culture from the intraoperative debridement specimen was negative. However, histopathology of the resected tissue was compatible with a mycotic aneurysm. Therefore, cefepime 2 g daily — an empirical antibiotic — was administered for 10 days. White blood cell count became normalized and C-reactive protein level reduced to 1.7 mg/dL. The patient's condition remained stable, and a CT scan on postoperative day 10 showed patency of both the autologous and ePTFE grafts (Fig. 3). The patient was ambulatory and was discharged from our hospital on postoperative day 20.

Discussion

The treatment strategy for mycotic aneurysms comprises debridement of the infected tissue and reconstruction of vascular continuity. We employed an extra-anatomical crossover bypass to avoid any foreign material in the infected region together with the use of an autologous graft to reconstruct the right ⅡA. Patency of the extra-anatomical bypass has been reported to be slightly low. Once the graft is occluded in the future, patency of the ⅡA will be important as a collateral to the lower extremity. Therefore, we believed that reconstruction of the ⅡA was mandatory. Furthermore, precluding the existence of the transected end could avoid the future formation of pseudoaneurysm.

Several materials for reconstruction have been evaluated, including *in situ* graft replacement using antibiotic-coated prosthetic grafts[2], cryopreserved human allografts[3], autogenous femoro-popliteal vein grafts[4], and autologous arterial grafts[5]. However, the most effective material is yet to be determined.

A cryopreserved human allograft is a good alternative to a synthetic graft for arterial reconstruction[3]; however, human allografts are not easily available. The use of autologous venous grafts (e.g., femoral, popliteal, and saphenous veins) has been reported[6]. Reinfection or aneurysmal dilatation was not observed by Daenens et al[6] after *in situ* reconstruction using the femoral veins to treat infrarenal aortic graft infections. However, serious post-surgical complications have been reported after using grafts from the femoral or popliteal veins and include the need for revision surgery due to major bleeding, above-the-knee amputation, graft limb occlusion, and late graft limb stenosis[4,7,8]. Severe venous stasis and acute compartment syndrome were also reported after the femoral and popliteal veins were harvested. The great saphenous vein has also been used as an alternative because harvesting it is less invasive, and subsequent venous stasis is mild. To accommodate for size discrepancies, the saphenous vein should be spliced. Reconstructions using

grafts from spiral and paneled saphenous veins are the most well-known procedures[9,10]. However, late aneurysmal degeneration has been reported[11]. These complications elucidate the limitations of using venous grafts for arterial reconstructions. Although autologous grafts may be tolerant to infection, venous grafts appear to have limited integrity and durability. The use of an autologous arterial graft would overcome these drawbacks. In our present case, an autologous graft from the contralateral EIA was used for domino reconstruction.

Anatomical limitations of this graft included its own length and diameter. An autologous graft from the EIA was previously used for the reconstruction of the subclavian artery in which the size and length were compatible[5]. However, in the present case, its limited length did not allow us to anatomically bypass the occluded right EIA. Therefore, extraanatomical bypass was employed. Other drawbacks of domino reconstruction include infection, bleeding, and potential occlusion of the synthetic graft used to reconstruct the iliac artery where no pathology was previously present. However, the theoretical advantages of infection resistance, durability, and the potential long-term patency of this type of viable arterial reconstruction may outweigh these drawbacks.

In this case, ilio-deep femoral bypass was not mandatory, because ischemic symptom was minimal, such as intermittent claudication. Avoiding the use of synthetic material as possible could be a good strategy during infection condition. Delayed bypass for right leg ischemia could be a good option.

In conclusion, an autologous graft from the contralateral iliac artery was harvested and replaced with an ePTFE graft. The autologous graft was used for *in situ* domino reconstruction to successfully treat a mycotic aneurysm of the common iliac artery.

Acknowledgement

All authors have no COI to declare regarding the present study.

I would like to thank Shoichi Terakawa for contributing to the reconstruction and analysis of the images.

References

1. Sörelius K, Budtz-Lilly J, Mani K, et al. Systematic review of the management of mycotic aortic aneurysms. Eur J Vasc Endovasc Surg 2019;58:426-435.
2. Hayes PD, Nasim A, London NJ, et al. In situ replacement of infected aortic grafts with rifampicin-bonded prostheses: the Leicester experience (1992 to 1998). J Vasc Surg 1999;30:92-98.
3. Brown KE, Heyer K, Rodriguez H, et al. Arterial reconstruction with cryopreserved human allografts in the setting of infection: a single-center experience with midterm follow-up. J Vasc Surg 2009;49:660-666.
4. Ehsan O, Gibbons CP. A 10-year experience of using femoro-popliteal vein for re-vascularisation in graft and arterial infections. Eur J Vasc Endovasc Surg 2009;38:172-179.
5. Murakami T, Tokuda T, Nishimura S, et al. Successful treatment of Staphylococcus schleiferi infection after aortic arch repair: in situ aortic arch replacement and domino reconstruction of the debranching graft using autologous iliac artery. Acta Med Okayama 2020;74:251-255.
6. Daenens K, Fourneau I, Nevelsteen A. Ten-year experience in autogenous reconstruction with the femoral vein in the treatment of aortofemoral prosthetic infection. Eur J Vasc Endovasc Surg 2003;25:240-245.
7. Ali AT, Modrall JG, Hocking J, et al. Long-term results of the treatment of aortic graft infection by in situ replacement with femoral popliteal vein grafts. J Vasc Surg 2009;50:30-39.
8. Dorweiler B, Neufang A, Chaban R, et al. Use and durability of femoral vein for autologous reconstruction with infection of the aortoiliofemoral axis. J Vasc Surg 2014;59:675-683.
9. van Zitteren M, van der Steenhoven TJ, Burger DH, et al. Spiral vein reconstruction of the infected abdominal aorta using the greater saphenous vein: preliminary results of the Tilburg experience. Eur J Vasc Endovasc Surg 2011;41:637-646.
10. Mallios A, Boura B, Alomran F, et al. A new technique for reconstruction of the aortic bifurcation with

saphenous vein panel graft. J Vasc Surg 2014;59:511-515.
11. Schwarcz TH, Nypaver TJ. Paneled saphenous vein graft repair of an iliac artery injury in a contaminated abdomen: late complication of aneurysmal degeneration illustrating the need for continued surveillance. J Vasc Surg 2017;66:e38-39.

Instructions for Authors

The Osaka City Medical Journal will consider the publication of any original manuscript, review, case report, or short communication. Articles should be in English.

Manuscript submission. Manuscripts should be sent to the Editor, Osaka City Medical Journal, Osaka City Medical Association, Graduate School of Medicine, Osaka Metropolitan University, 1-4-3 Asahimachi, Abeno-ku, Osaka 545-8585, Japan; phone and fax 06-6645-3782; e-mail gr-med-shiigakukai@omu.ac.jp

The Journal accepts only manuscripts that contain material that has not been and will not be published elsewhere. Duplicate publication of scientific data is not permitted. If closely related papers might be considered to be duplicate publications, the possible duplicate should be submitted with the manuscript and the authors should explain in their covering letter what is original in the submitted paper. Submit three copies of the manuscript (two of which may be photocopies) together with CD-R or DVD-R containing the body text, tables and figures. The manuscript should be prepared by Microsoft Word or its compatible software (doc or docx). Acceptable formats for figures are JPG or TIF. Use only 12-point font size and a standard serif font. Double-space throughout the manuscript and use standard-sized (ISO A4, 212×297 mm) white bond paper. Make margins at least 25 mm wide on all sides. Number pages consecutively starting with the title page and ending with the reference list. Begin each of these sections on a separate page: title page, abstract, text, acknowledgements, references, tables (each one separate), and figure legends. Do not use abbreviations in the title or abstract and limit their use in the text, defining each when it first appears. Manuscripts should meet the requirements outlined below to avoid delay in review and publication. Authors whose native language is not English must seek the assistance of a native English speaker who is familiar with medical sciences. Please attach the certificate from the person(s) who edit the manuscript. Some minor editorial revision of the manuscript will be made when the editorial committee considers it necessary.

Title page. All submissions must include a title page. The full title of the paper, should be concise, specific, and informative, and should contain the message of the paper without being in sentence form. Next, include the full names and academic affiliations of all authors, and indicate the corresponding author, address, phone, fax, and e-mail address. Give a running title (not to exceed 50 characters including spaces), and three to five key words. Last, give the word count for text only, exclusive of title, abstract, references, tables, and figure legends.

Structured abstract. The abstract of 250 words or less should consist of four paragraphs headed **Background, Methods, Results,** and **Conclusions.**

Text. Full papers about experiments or observations may be divided into sections headed **Introduction, Methods, Results,** and **Discussion.**

Tables. Each table should be typed on a separate sheet in characters of ordinary size, double-spaced (with at least 6 mm of white space between lines). Each table must have a title and should be assigned an Arabic numeral ('Table 3'). Vertical rules should not be used.

Figures. For black-and-white figures, submit three original glossy prints or laser-quality proofs and three photocopies of each. One transparency and three color prints should be submitted of each color figure. Label the front of figures with the figure number. Indicate on the back of each figure the first author, the first few words of the manuscript title, and the direction of the top of the figure (if needed). Photomicrographs should have scale markers that indicate the magnification. Provide figure legends on a separate page, double-spaced, immediately after the tables. All illustrations and graphs, to be referred to as figures, should be numbered in Arabic numerals ('Fig. 2' etc.). The approximate position of each figure in the text should be indicated in the right margin of the manuscript. Illustrations in full color are accepted for publication if the editors judge that color is necessary, with the cost paid by the author.

References. Reference must be double-spaced and numbered consecutively in the order cited in the text. When listing references, follow the style of the Uniform Requirements (http://www.icmje.org/) and abbreviate names of journals according to PubMed (http://www.ncbi.nlm.nih.gov/sites/netrez). List all authors up to three; when there are four or more, list the first three and use et al.

Examples of reference style

1. Priori SG, Schwartz PJ, Napolitano C, et al. Risk stratification in the long-QT syndrome. N Engl J Med 2003;348:1866-1874.
2. Schwartz PJ, Priori SG, Napolitano C. The long-QT syndrome. In: Zipes DP, Jalife J, editors. Cardiac electrophysiology: from cell to bedside. 3rd ed. Philadelphia: W.B. Saunders; 2000. pp. 597-615.

Proofs. One set of proofs together with the original manuscript will be sent to the author, to be carefully checked for any essential changes or printer's errors. The author is requested to return the corrected proofs within 48 h of their receipt.

Short communications and case reports.

1. A short communication should have between 1500 and 2000 words, including the abstract. This word count is equivalent to about four double-spaced manuscript pages.
2. The original and two copies including three sets of figures and tables should be sent to the Editorial Office.

Manuscript submission fee. A nonrefundable fee of 10,000 JPY is due on submission of original manuscripts, case reports, and short communications. A manuscript returned beyond six months of the date of the initial decision will be considered a new submission.

Page charges. A standard publication fee of 100,000 JPY will be applied for each accepted paper. Authors are also required to pay page charge of 10,000 JPY per printed page.
Ex) If your article has 10 pages, the amount of fee is 100,000 JPY+10 pages×10,000 JPY=200,000 JPY.

Reprints. If you were interested in ordering reprints of your article, we accept at least 50 full-color copies. Authors are required to pay page charge of 100 JPY per printed page. Ex) If you request 60 copies for 10-page article, the amount of fee is 100 JPY×10 pages×60 copies=60,000 JPY.

Studies of human subjects. It is the responsibility of the authors to ensure that any clinical investigation they did and report in manuscripts submitted to the Osaka City Medical Journal are in accordance with the Declaration of Helsinki (http://www.wma.net).

Animal studies. It is the responsibility of the authors to ensure that their experimental procedures are in compliance with the "Guiding Principles in the Care and Use of Animals" (http://www.the-aps.org/pub_affairs/humane/pa_aps_guiding.htm) published each month in the information for authors of the American Journal of Physiology.

Conflict of Interest (COI) Disclosure.

1. It is the responsibility of the authors to disclose any COI by signing the form.
2. If the authors have no conflicts, please state "All authors have no COI to declare regarding the present study" in the Acknowledgements.
   Authors are required to disclose any relationships with company or organization (such as funds, consultancy fee, grant, fee for speaking, stock or shares). At the time of initial submission, the corresponding author is responsible for obtaining conflict of interest information from all authors.

[Revised: June 8, 2021]

COPYRIGHT TRANSFER AND STATEMENT OF ORIGINALITY

We approve the submission of this paper to the Osaka City Medical Association for publication and have taken to ensure the integrity of this work. We confirm that the manuscript is original and does not in whole or part infringe any copyright, violate any right of privacy or other personal or priority right whatever, or falsely designate the source of authorship, and that it has not been published in whole or in part and is not being submitted or considered for publication in whole or in part elsewhere (abstracts excluded).
We agree to transfer copyright the manuscript entitled

_____

_____

to the Osaka City Medical Association upon its acceptance for publication.

Write clearly and signature

(Author: print or type)	(Signature)	(Date)
_____	_____	_____
(Author: print or type)	(Signature)	(Date)
_____	_____	_____
(Author: print or type)	(Signature)	(Date)
_____	_____	_____
(Author: print or type)	(Signature)	(Date)
_____	_____	_____
(Author: print or type)	(Signature)	(Date)
_____	_____	_____
(Author: print or type)	(Signature)	(Date)
_____	_____	_____
(Author: print or type)	(Signature)	(Date)
_____	_____	_____
(Author: print or type)	(Signature)	(Date)
_____	_____	_____
(Author: print or type)	(Signature)	(Date)
_____	_____	_____

OCMJ for Conflict of Interest (COI) Disclosure Statement

The purpose of this form is to provide readers of your manuscript with information about your other interests that could influence how they receive and understand your work. The form is designed to be completed and stored electronically. Each author should submit this form and is responsible for the accuracy and completeness of the submitted information.

1. 1) Have you accepted from a sponsor or any company or organization (More than 1,000,000 JPY per year from a specific organization) ? (Please circle below)
   (1) Funds ? ····· Yes / No
   (2) Consultancy fee ? ····· Yes / No
   (3) Any grant ? ····· Yes / No
   (4) Fee for speaking ? ····· Yes / No

   2) Do you hold any stock or shares related to the manuscript ?
   (1) Directly ? ····· Yes / No
   (2) Indirectly, via family members or relatives ? ····· Yes / No

   3) If any of above items are “yes”, please provide detailed information below.

2. If none of the above apply and there is no COI please clearly state “All authors have no COI to declare regarding the present study”.

Manuscript Title:

Name / Signature_____ **Date**_____

Manuscript Identifying Number (if you know it):

Editorial Committee

The volumes and issues published in 1954-2018 were as follows: Vol 1 (one issue), Vols 2-5 (2 issues, each), Vols 6-7 (one issue, each), Vols 8-9 (2 issues, each), Vol 10 (one issue), Vol 11 (2 issues), Vol 12 (one issue), Vol 13 (2 issues), Vols 14-20 (one issue, each), Vol 21 (2 issues), Vol 22 (one issue), Vols 23-65 (2 issues, each), Vol 66 (one issue), Vol 67-69 (2 issues, each)

Publisher : Osaka City Medical Association,
Graduate School of Medicine, Osaka Metropolitan University
1-4-3 Asahimachi, Abeno-ku, Osaka 545-8585, Japan